MR No. L5D12a

NATIONAL ADVISORY COMMITTEE FOR AERONAUTICS

WARTIME REPORT

ORIGINALLY ISSUED
April 1945 as
Memorandum Report L5D12a

TESTS OF 0.14-SCALE MODELS OF THE CONTROL SURFACES OF ARMY PROJECT MX-511 IN ATTITUDES SIMULATING SPINS

By H. Page Hoggard, Jr. and John R. Hagerman

Langley Memorial Aeronautical Laboratory
Langley Field, Va.

WASHINGTON

MR No. L5D12a

NATIONAL ADVISORY COMMITTEE FOR AERONAUTICS

MEMORANDUM REPORT

for the

Army Air Forces, Air Technical Service Command

TESTS OF 0.14-SCALE MODELS OF THE CONTROL SURFACES OF ARMY PROJECT MX-511 IN ATTITUDES SIMULATING SPINS

By H. Page Hoggard, Jr. and John R. Hagerman

SUMMARY

Tests of 0.14-scale models of the partial-span wing and the isolated tail of the Bell XP-83 airplane (Army Project MX-511) have been made in the Langley 4-by 6-foot tunnel to determine the aerodynamic characteristics in attitudes simulating spin conditions. The tests were made at a Mach number of about 0.095.

The slope of the curve of aileron hinge moment against angle of attack increases negatively as the angle of attack of the wing is increased. At the higher angles of attack the slope of the curve of aileron hinge moment against aileron deflection is more negative for small aileron deflections even though the aileron hinge-moment increment from 25° to -25° aileron deflections is practically constant over the angle-of-attack range. The data presented indicate that in spin attitudes the yawing moment produced by the aileron is practically as much as the rolling moment.

The elevator hinge-moment increment from 25° to -25° elevator deflections is practically constant over the angle-of- attack range and the slope of the curve of elevator hinge moment against angle of attack increases negatively as the angle of attack of the horizontal tail is increased. The elevator hinge-moment and lift-curve slopes of the isolated-tail model show close agreement with those of the complete model.

As the angle of attack is increased the drag produced by elevator deflection increases while the lift produced by elevator deflection decreases. The elevator deflection has large effects on rudder hinge moments at $\alpha_t = 20.5°$ and angle of yaw and rudder deflection of like signs. No consistent effect of elevator deflection on rudder hinge moment is shown at $\alpha_t = 50.4°$, except that negative elevator deflec-

tions usually gave the largest rudder hinge moments for the yawed conditions.

INTRODUCTION

In view of the results of spin tests of a model of the Bell XP-83 airplane (Army Project MX-511) conducted in the Langley 20-foot free-spinning tunnel, it was deemed necessary to determine the hinge-moment characteristics of the control surfaces of the 0.14-scale model of the Bell XP-83 airplane in attitudes simulating spins.

In order to obtain the necessary control-surface hinge-moment data, 0.14-scale models of the left wing panel and of the isolated tail unit were tested in the Langley 4- by 6-foot tunnel. The hinge-moment data obtained are presented herein, along with the lift and drag data obtained from the same tests. It is planned to use the data presented herein in the estimation of stick and pedal forces during the steady spin and for spin recovery. Complete ranges of aileron, elevator, and rudder deflection over wide ranges of angle of attack and yaw simulating spin conditions were investigated.

COEFFICIENTS AND SYMBOLS

The results of the tests are presented as standard non-dimensional NACA coefficients of forces and moments as follows:

C_{L_u} uncorrected lift coefficient of test panel $\left(\frac{L_u}{qS_w}\right)$

C_{L_w} corrected lift coefficient of test panel $\left(\frac{L_w}{qS_w}\right)$

C_{L_t} horizontal tail lift coefficient $\left(\frac{L_t}{qS_t}\right)$

C_{D_u} uncorrected drag coefficient of test panel $\left(\frac{D_u}{qS_w}\right)$

C_{D_w} corrected drag coefficient of test panel $\left(\frac{D_w}{qS_w}\right)$

C_{D_t} horizontal tail drag coefficient $\left(\frac{D_t}{qS_t}\right)$

C_l rolling-moment coefficient of complete wing $\left(\frac{L}{qS'b'}\right)$

C_n yawing-moment coefficient of complete wing $\left(\frac{N}{qS'b'}\right)$

C_{h_a} aileron hinge-moment coefficient $\left(\frac{H_a}{qb_a\bar{c}_a^2}\right)$

$C_{h_{el}}$ left elevator hinge-moment coefficient $\left(\frac{H_{el}}{qb_{el}\bar{c}_e^2}\right)$

C_{h_r} rudder hinge-moment coefficient $\left(\frac{H_r}{qb_r\bar{c}_r^2}\right)$

where

L_u uncorrected lift force on test panel

L_w corrected lift force on test panel

L_t lift force on horizontal tail

D_u uncorrected drag force on test panel

D_w corrected drag force on test panel

D_t drag force on tail

L rolling moment about the wind axis, positive when it tends to raise the left wing tip (ft-lb)

N yawing moment about the wind axis, positive when it tends to advance the left wing tip (ft-lb)

H_a aileron moment about the aileron hinge axis, positive when it tends to depress the aileron trailing edge (ft-lb)

H_{el} left elevator moment about the elevator hinge axis, positive when it tends to depress the elevator trailing edge (ft-lb)

H_r rudder moment about the rudder hinge axis, positive when it tends to deflect the rudder trailing edge to the left (ft-lb)

q dynamic pressure (lb/sq ft) $\left(\frac{\rho V^2}{2}\right)$

ρ mass density of air (slugs/cu ft)

V airspeed (ft/sec)

S_w area of partial-span wing (sq ft)

S_t area of horizontal tail (sq ft)

S' area of wing on complete model (sq ft)

b' span of wing on complete model (ft)

b_a span of aileron along hinge axis (ft)

$\bar{c}_a$ root-mean-square chord of aileron behind hinge axis (ft)

b_{el} span of left elevator along hinge axis (ft)

$\bar{c}_e$ root-mean-square chord of elevator behind hinge axis (ft)

b_r span of rudder along hinge axis (ft)

$\bar{c}_r$ root-mean-square chord of rudder behind hinge axis (ft)

and

α_w angle of attack of test panel, referred to chord line at station 26.55 (degrees) (see fig. 1)

α_t angle of attack of tail unit, referred to reference line of dummy fuselage (degrees) (see fig. 3)

ψ_t angle of yaw, angle between model plane of symmetry and relative wind (degrees)

δ_a aileron deflection with respect to wing chord line, positive with trailing edge down (degrees)

δ_e elevator deflection with respect to stabilizer chord line, positive with trailing edge down (degrees)

δ_r rudder deflection with respect to chord line of fin, positive with trailing edge deflected to left (degrees)

i_t angle of chord plane of stabilizer relative to reference line of fuselage (-2.66°)

$\Delta C_{L'_{\delta_a}}$ one-half of the increment of uncorrected lift coefficient caused by deflection of the aileron on the model as tested (see note on page 6)

$\Delta C_{D'_{\delta_a}}$ one-half of the increment of uncorrected drag coefficient caused by deflection of the aileron on the model as tested (see note on page 6)

ΔC_{L_t} increment of tail lift coefficient for a given elevator deflection

ΔC_h increment of hinge-moment coefficient for a given surface deflection (with subscripts a, el, and r to denote aileron, left elevator, and rudder, respectively)

$$C_{l_{\alpha_w}} = \left(\frac{\partial C_{L_w}}{\partial \alpha_w}\right)_{\delta_a}$$

$$C_{L_{\alpha_t}} = \left(\frac{\partial C_{L_t}}{\partial \alpha_t}\right)_{\delta_e}$$

$$C_{l_{\delta_e}} = \left(\frac{\partial C_{L_t}}{\partial \delta_e}\right)_{\alpha_t}$$

$$C_{h_{\alpha_w}} = \left(\frac{\partial C_{h_a}}{\partial \alpha_w}\right)_{\delta_a}$$

$$C_{h_{\delta_a}} = \left(\frac{\partial C_{h_a}}{\partial \delta_a}\right)_{\alpha_w}$$

$$C_{h} \quad \left(\frac{\partial C_{h_{el}}}{\partial \alpha_t}\right)_{\delta_e}$$

where the subscripts outside the parentheses indicate the factors held constant during measurement of the parameters

$C_{h_{\delta_e}} = \left(\frac{\partial C_{h_{el}}}{\partial \delta_e}\right)_{a_t}$

$\frac{\partial C_m}{\partial i_t}$ change in pitching-moment coefficient of complete model of the airplane per degree change in stabilizer setting

$\frac{\partial C_m}{\partial \delta_e}$ change in pitching-moment coefficient of complete model of the airplane per degree change in elevator deflection

Note: Because the model of the wing panel was tested as a reflection-plane model, the deflection of one aileron will have the same aerodynamic effect on the model as the deflection of two ailerons in the same direction on a complete wing of the same plan form as the model plus its image. All increments of forces caused by aileron deflection are therefore twice those that would be obtained by deflecting only one aileron. This fact is noted on figures 7 and 8.

MODELS AND APPARATUS

The model of the partial-span left wing was composed of the tip and aileron assembly supplied by the Bell Aircraft Corporation for the investigation of the stability and control characteristics. A drawing of the model is presented in figure 1. The panel, from station 0 to the inboard end of the aileron, was made at the Langley Laboratory from templets supplied with the model, and was attached to the tip with steel straps. The complete model wing has a geometric twist of -2-1/4°. The partial-span model, for construction simplicity, was built with 0° twist between stations 0 and 17.850 (inboard end of aileron). This deviation in construction should have a negligible effect on the aileron characteristics above the stall. The aileron gap was sealed. Aileron hinge moments were read by means of an electrical strain gage. The location of the model in the Langley 4- by 6-foot wind tunnel is shown in figure 2. The geometric characteristics of the wing panel and aileron are presented in table I.

The model of the isolated tail unit was composed of the complete tail assembly supplied by the Bell Aircraft Corporation. The extended-span flat-sided rudder was used. A dummy fuselage, or fairing, was added by the Langley Laboratory, as shown in figure 3, to simulate a portion of the actual fuselage. The elevator and rudder gaps were not sealed. Elevator hinge moments were measured with an electrical strain gage on the left elevator only. Rudder hinge moments were also

read by means of an electrical strain gage. The position of the model in the Langley 4- by 6-foot wind tunnel is illustrated in figure 4. The strut supporting the fork and model was covered by a streamline fairing which was fastened to the tunnel wall. The strut itself was mounted on the balance system so that lift and drag forces could be read. The angle of attack of the model was changed by an electrical drive from outside the tunnel; the system was designed to give a range from 0° to 70°. The yaw tests were run by manually turning the outer end of the support strut while checking the angle with an inclinometer. A three-quarter top-view photograph is presented in figure 5. The geometric characteristics of the horizontal and vertical tails are presented in table II.

When the model of the tail was received from the Langley 8-foot high-speed tunnel, it was found to have a transition strip of No. 60 carborundum grains glued to the stabilizer surface at the 0.17 chord station over the entire stabilizer span. The transition strip was not removed since it probably would have little, if any, effect at the attitudes being investigated.

TESTS AND RESULTS

Test conditions.- The tests of the partial-span left wing panel were made in the Langley 4- by 6-foot tunnel at a dynamic pressure of 13 pounds per square foot for angles of attack up to 35°, and at 10 pounds per square foot for angles of attack from 30° to 67°. The values of q of 13 and 10 pounds per square foot correspond to test Reynolds numbers of about 700,000 and 610,000, respectively, based on the average chord, for the wing panel tested, of 1.04 feet. Because of the turbulence factor of 1.93 for the 4- by 6-foot tunnel, the effective Reynolds numbers are 1,350,000 and 1,178,000, respectively.

The tests of the isolated tail were also made in the Langley 4- by 6-foot tunnel at a dynamic pressure of 13 pounds per square foot, which corresponds to a Mach number of about 0.095. Tests were run through a yaw range from -35° to 35° at constant angles of attack of the fuselage reference line of 20° and 50° with elevators and rudder at various deflections simulating their probable positions in a spin. The control surface tabs were neutral for all tests. Pitch tests were also run through an angle-of-attack range of 0° to 70°, with the elevator set at various deflections, and the rudder set at 0° for all tests. The horizontal-tail incidence was -2.66° with respect to the fuselage reference line for all tests. The test Reynolds number, based on the average chord of the horizontal tail of 0.563 feet, and a dynamic pressure of 13

pounds per square foot, is 370,000, and the effective Reynolds number is 714,000.

A dummy tail block (with tail surfaces removed) supplied by the Bell Aircraft Corporation was attached to the dummy fuselage, or fairing, and tested through a yaw range of -35° to 10° at constant angles of attack of the fuselage reference line of 20° and 50°. Also a pitch test was run through an angle-of-attack range of 0° to 70° at zero yaw.

Corrections.- The data on the partial-span wing have been corrected, by the method described in reference 1, for the influence of jet boundaries. The jet-boundary corrections for the partial-span wing were applied as follows:

$$\Delta\alpha_w = 1.193 \; C_{L_u}$$

$$\Delta C_{L_w} = -0.020 \; C_{L_u}$$

$$\Delta C_{D_{i_w}} = 0.0158 \; C_{L_u}^2$$

$$\Delta C_{h_a} = 0.00313 \; C_{L_u}$$

These corrections were added to the partial-span wing test values.

The rolling and yawing moments for the deflection of one aileron on the wing of the complete model airplane were estimated by use of the following equations:

$$C_l = 0.2265 \; \Delta C_{L'_{\delta_a}}$$

and

$$C_n = -0.284 \; \Delta C_{D'_{\delta_a}} + 0.003 \left(C_{L_u}\right)_{\delta_a = 0^\circ} \Delta C_{L'_{\delta_a}}$$

If it is desired to convert the data of figures 7 and 8 to the plan form of the complete airplane, the increments of lift and drag caused by aileron deflection should be divided by 2, and all angles of attack should be corrected by adding the increment $\Delta\alpha_w = -0.400 \; C_{L_w}$.

The data for the isolated tail have been corrected for the influence of the jet boundaries. The jet-boundary correction was applied as follows:

$$\Delta\alpha_t = 0.9109 \; C_{L_t}$$

This correction was added to the test values. The correction to the induced drag caused by the jet boundaries was found to be negligible. The lift and drag data for the tail surfaces alone were obtained by subtracting the values for the dummy fuselage alone (figs. 15 and 16) from the values obtained from tests of the dummy fuselage with tail surfaces. Thus, the lift and drag characteristics presented for the tail surfaces still include the fuselage-tail interference, but not the direct fuselage forces. The pressure difference between the inside of the strut fairing and the atmosphere outside the tunnel necessitated a correction to the lift data which was obtained by calibration. The corrections to the hinge moments of the rudder and elevator were found negligible and were not applied.

Test procedure.- The 0.14-scale partial-span wing model was mounted in the tunnel (fig. 2) with station 0 adjacent to the tunnel wall, which thereby acted as a reflection plane. The model was supported entirely by the balance frame with a small clearance at the tunnel wall so that all forces and moments acting on the model could be measured. Since the 0 station of the wing is not on the center line of the airplane, the lift and drag presented herein are for two ailerons deflected in the same direction on a wing of aspect ratio 5.69 having an area of 6.20 square feet, including the reflection image, instead of for one aileron on the complete model which has a wing of aspect ratio 6.52 with an area of 8.45 square feet. This difference in aspect ratio is thought to have a negligible effect on the aileron hinge moment, particularly at high angles of attack.

The electric angle-of-attack drive is designed to give a range of approximately 40°. For this reason it was necessary to run the tests from 0° to 35° for all aileron deflections, and then to repeat the tests for some aileron deflections with the angle-of-attack range shifted to give 30° to 67°. The accuracy of resetting the deflections is indicated by the double points on the curves at $\alpha_w = 30°$ and 35° in figures 6, 7, and 8. The tests were run at constant aileron deflections, except for a slight strain-gage deflection, in 2° increments of angle of attack through the stall, and then in 5° increments up to 65°, the last step being 2° to reach 67°. The aileron deflection range was from neutral to ±25° in 5° increments.

The yaw tests for constant elevator deflections of -25° and 25° were run in 5° increments of yaw from 0° to +35° and from 0° to -35° while holding angle of attack and rudder deflections constant. The yaw tests run at a constant elevator deflection of 15° were made in 5° steps from 0° to 10° and from 0° to -35° while holding angle of attack and rudder deflections constant. The control-surface deflections varied slightly because of strain-gage deflection.

DISCUSSION

Partial-Span Wing Tests

The partial-span wing data presented in this paper are being used in estimating stick forces (to be published) on the ailerons at high angles of attack simulating spin conditions (fig. 6). Lift, drag, rolling-moment, and yawing-moment characteristics are also presented (figs. 7, 8, 9, and 10, respectively).

Aileron hinge moments.- The values of $C_{h_{\alpha_w}}$ and $C_{h_{\delta_a}}$, as read over a small range of α_w and δ_a at low angles of attack (fig. 6), are -0.0015 and -0.0036, respectively. Values of $C_{h_{\alpha_w}}$ and $C_{h_{\delta_a}}$, as determined from tests of the complete model in the Langley 7- by 10-foot wind tunnel (unpublished), are -0.0020 and -0.0040, respectively. The close agreement of the parameter values at low angles of attack for the complete model wing and the partial-span wing of slightly different aspect ratio indicates that the differences in aspect ratio, wind tunnel, and test procedures have little effect on the hinge-moment parameter values for this particular case.

The curves of figure 6 indicate that the slope, $C_{h_{\alpha_w}}$, is increased from -0.0015 at low angles of attack to about -0.0070 at angles of attack between 40° and 50°. The slope, $C_{h_{\delta_a}}$, for small deflections is increased from -0.0036 at low angles of attack to about -0.0100 at high angles of attack. The total increment in C_{h_a} between deflections of ±25°, however, is fairly constant for the whole angle-of-attack range.

Wing lift and drag.- No plan-form corrections have been applied to the lift and drag data in figures 7 and 8, which therefore represent the deflection of two ailerons in the same direction on a wing of aspect ratio 5.69.

The slope of the lift curve, $C_{L_{\alpha_w}}$, for the complete-model wing with fuselage and canopy was found to be 0.072 when read over a range of $\alpha_w = \pm 6°$ (unpublished). The slope of the lift curve for fuselage and canopy only is very low and therefore the value above may be considered as that for the wing alone. The partial-span wing data gave a $C_{L_{\alpha_w}}$ value of 0.067 and application of the plan-form corrections given previously would increase this slope to about 0.069 which compares

favorably with the complete-wing value of 0.072.

Aileron rolling and yawing moments.- By means of the equations given previously, the uncorrected data used to compute the corrected data of figures 7 and 8 were also used to compute the rolling- and yawing-moment coefficients for the deflection of one aileron on a wing of aspect ratio 6.52, for comparison with the data from the complete model (unpublished). These rolling- and yawing-moment coefficients are plotted in figures 9 and 10 against aileron deflection.

A comparison of the rolling-moment characteristics of figure 9 with data from the complete model indicated fair agreement. The agreement shown is thought to be fairly good considering the mathematical manipulations involved in computing rolling-moment coefficients from the lift data of the present partial-span tests.

A similar estimation and comparison was made for the yawing-moment characteristics resulting from aileron deflection on the complete model (fig. 10). The agreement is fairly good for negative aileron deflections, but not for positive deflections. A lack of agreement might be expected because of the small increments of drag and the difficulty of determining the correct spanwise lever arm at which this small increment of drag may be considered to act.

Although the computed rolling and yawing moments cannot be considered very accurate, the data indicate that in spin attitudes the yawing moment produced by the aileron is as much as or more than the rolling moment produced.

Isolated Tail Tests

The isolated tail hinge-moment data presented in this paper (figs. 11 and 12) were obtained for use in estimating stick and pedal forces (to be published) at angles of attack and yaw simulating spin attitudes. Lift and drag characteristics were also obtained and are presented in figures 13 and 14.

Elevator hinge moments.- From tests of the complete model (unpublished), the value of $C_{h_{\alpha_t}}$ is approximately 0.0020, and $\Delta C_{h_{e_l}}$ was found to be approximately -0.028 for 10° elevator deflection. The values taken from the present data in the unstalled condition (fig. 11) were $C_{h_{\alpha_t}} = 0.0020$ and $\Delta C_{h_{e_l}} = -0.030$ for $\delta_e = 15°$. For the present tests transition was fixed while for the complete-model tests it was free.

The curves for $\delta_e = 0°$ and $-25°$, in figure 11, appear to fall together in the stalled range between $\alpha_t = 24°$ and $32°$. The value of $C_{h_{\alpha_t}}$ at $\delta_e = 0°$ changed from 0.0020 at $\alpha_t = 0°$ to about -0.0120 at $\alpha_t = 50°$. The elevator hinge-moment increment resulting from changing the deflection of the elevator from $-25°$ to $25°$ increased between $\alpha_t = 0°$ and $15°$, decreased from $15°$ to about $30°$ α_t, and then increased again until at $\alpha_t = 60°$ the increment was about equal to that at $\alpha_t = 0°$.

For yaw tests at constant α_t (fig.12) the left elevator hinge-moment curves generally have a negative slope with angle of yaw. This slope becomes fairly steep for negative angles of yaw with $\alpha_t = 50.4°$. The negative slope of $C_{h_{el}}$ against ψ_t may be caused by the dihedral angle of the horizontal tail, which, at positive angles of yaw, gives the left horizontal tail a positive increment of α_t; and, since $C_{h_{\alpha_t}}$ is generally negative, the positive increment of α_t causes a negative increment of $C_{h_{el}}$.

Changing rudder deflection from minus to plus generally increased the negative value of $C_{h_{el}}$ for all the values of ψ_t, α_t, and δ_e tested.

Rudder hinge moments.- At $\alpha_t = 20.5°$ (fig. 12) the rudder hinge-moment curves generally have a negative slope with angle of yaw. With angle of yaw and rudder deflection of opposite sign, the elevator deflection has practically no effect on rudder hinge moments at $\alpha_t = 20.5°$ for large angles of yaw. With like signs for ψ_t and δ_r the elevator deflection has a large effect on rudder hinge moments. A negative increment in δ_e generally produces a positive increment in C_{h_r} for negative values of δ_r and a negative increment in C_{h_r} for positive values of δ_r. With $\alpha_t = 50.4°$ no consistent effect of elevator deflection on rudder hinge moments

is shown, except that negative elevator deflections usually result in slightly larger rudder hinge moments at high angles of yaw. No data are available for comparison of the rudder hinge-moment characteristics in yaw presented here with those of the rudder on the complete model, because the complete model data were obtained at angles of attack below the stall.

The curves, in general, show the large effect of the deflection of one control surface on the hinge moments of the other, especially the large effect of elevator deflection on rudder hinge moment.

Tail lift and drag.- The lift and drag data are presented for the tail surfaces (including fuselage-tail interference) in figures 13 and 14.

The slope of the unstalled ($\alpha_t = 0^\circ$ to 10°) lift curve with elevator neutral was found to be 0.056 from the data shown in figure 13. An equal value of $C_{L_{\alpha_t}}$ was obtained by calculation from the value $\frac{\partial C_m}{\partial i_t} = -0.0243$ obtained in the complete model tests (assuming the q ratio at the tail equal to one). The complete model tests of reference 2 gave a value of $\frac{\partial C_m}{\partial \delta_e} = -0.0155$ which by the method of calculation discussed above gives $\frac{\partial C_{L_t}}{\partial \delta_e} = 0.036$. From the present data, the value of ΔC_{L_t} for an elevator deflection of 15° is 0.45, which if the variation is assumed linear would give $\frac{\partial C_{L_t}}{\partial \delta_e} = 0.030$.

From figure 13 the decreasing effect of elevator deflection on tail lift with increased angle of attack is obvious. The drag increment caused by elevator deflections, however, appears to increase with angle of attack.

The lift effectiveness of the elevator, $C_{L_{\delta_e}}$, increases with angle of yaw when $\alpha_t = 20.5^\circ$, while with $\alpha_t = 50.4^\circ$ the lift effectiveness decreases with angle of yaw (fig. 14) Rudder deflection had comparatively little effect on the value of C_{L_t}.

The drag at high angles of yaw and $\alpha_t = 20.5^\circ$ depends on both elevator and rudder deflections, and is smallest when both surfaces are deflected more nearly parallel to the relative wind. With $\alpha_t = 50.4^\circ$ the same tendency for lower drag with the surfaces deflected parallel to the relative wind exists, but is of smaller magnitude. At $\alpha_t = 20.5^\circ$ the drag, with surfaces at any combination of deflections, increased with angle of yaw, while at $\alpha_t = 50.4^\circ$ the drag remained nearly constant or decreased with angle of yaw.

Fuselage lift and drag.- The lift and drag characteristics of the dummy fuselage without the tail surfaces are presented in figures 15 and 16. It is to be noted that the interference effect of the strut and fork are included in these values.

The curve of lift against angle of attack in figure 15 shows the usual low slope value for a plain isolated fuselage, The drag curves in figures 15 and 16 show the usual increase in drag with both angle of attack and yaw.

CONCLUSIONS

From the results of test of 0.14-scale models of the Bell XP-83 control surfaces in the Langley 4- by 6-foot tunnel at attitudes simulating spin conditions, the following conclusions may be drawn:

1. The slope of the curve of aileron hinge moment against angle of attack increases negatively as the angle of attack of the wing is increased. The aileron hinge-moment increment from 25° to -25° aileron deflections is practically constant over the angle-of-attack range even though the slope of the curve of aileron hinge moment against aileron deflection is more negative for small aileron deflections at the higher angles of attack.

2. The data presented indicate that the aileron produces practically as much yawing moment as rolling moment when in spin attitudes.

3. The slope of the curve of elevator hinge moment against angle of attack increases negatively as the angle of attack of the horizontal tail is increased. The elevator hinge-moment increment from 25° to -25° elevator deflections is practically constant over the angle-of-attack range tested.

4. The lift-curve slope and the elevator hinge-moment slopes for the isolated-tail model and the complete model show close agreement.

5. The data presented indicate that the drag produced by elevator deflection increases as the angle of attack is increased while the lift produced by elevator deflection decreases.

6. At $\alpha_t = 20.5^\circ$, and angle of yaw and rudder deflection of like signs, the elevator deflection has large effects on rudder hinge moments. At $\alpha_t = 50.4^\circ$ no consistent effect of elevator deflection on rudder hinge moment is shown, except that negative elevator deflections usually gave the largest rudder hinge moments for the yawed conditions.

Langley Memorial Aeronautical Laboratory
National Advisory Committee for Aeronautics
Langley Field, Va.

REFERENCE

1. Swanson, Robert S., and Toll, Thomas A.: Jet-Boundary Corrections for Reflection-Plane Models in Rectangular Wind Tunnels. NACA ARR No. 3E22, 1943.

TABLE I

GEOMETRIC CHARACTERISTICS OF WING AND AILERON OF 0.14-SCALE MODEL OF THE BELL XP-83 AIRPLANE

	Complete span	Partial span
Area (partial span = model area + image area), sq ft	8.45	6.20
Average chord, ft	1.14	1.04
Span (partial span + image), ft	7.42	5.95
Aspect ratio (partial span + image)	6.52	5.69
Taper ratio	2.6:1	2.6:1
Single aileron area, sq ft	2.15	2.15
Single aileron span (along hinge axis), ft	1.453	1.453
Aileron root-mean-square chord, ft	.207	.207
Aileron balance area, sq ft	.69	.69
Ratio of aileron balance area to aileron area, percent	32.5	32.5
Aileron deflection range, deg	±25	±25

TABLE II

GEOMETRIC CHARACTERISTICS OF 0.14-SCALE MODELS OF THE BELL XP-83 HORIZONTAL AND VERTICAL TAIL SURFACES

Vertical tail:

Total area, sq ft	0.932
Span, ft	1.191
Aspect ratio	1.523
Angle of offset, degrees	0

Rudder:

Area, sq ft	0.274
Span, ft	1.431
Root-mean-square chord, ft	0.193
Ratio of balance area to rudder area	0.435
Ratio of rudder area to vertical tail area.	0.294
Average,chord, ft	0.191
Maximum deflection, degrees	±25

Horizontal tail:

Area, total, sq ft	1.470
Span, total, ft	2.610
Average chord, ft	0.563
Aspect ratio	4.650
Stabilizer dihedral, degrees	10

Elevator:

Percent elevator balance,	48
Area aft of hinge (one elevator), sq ft	0.195
Root-mean-square chord, ft	0.165
Maximum deflection, degrees	±25
Span along hinge axis (one elevator), ft	1.300

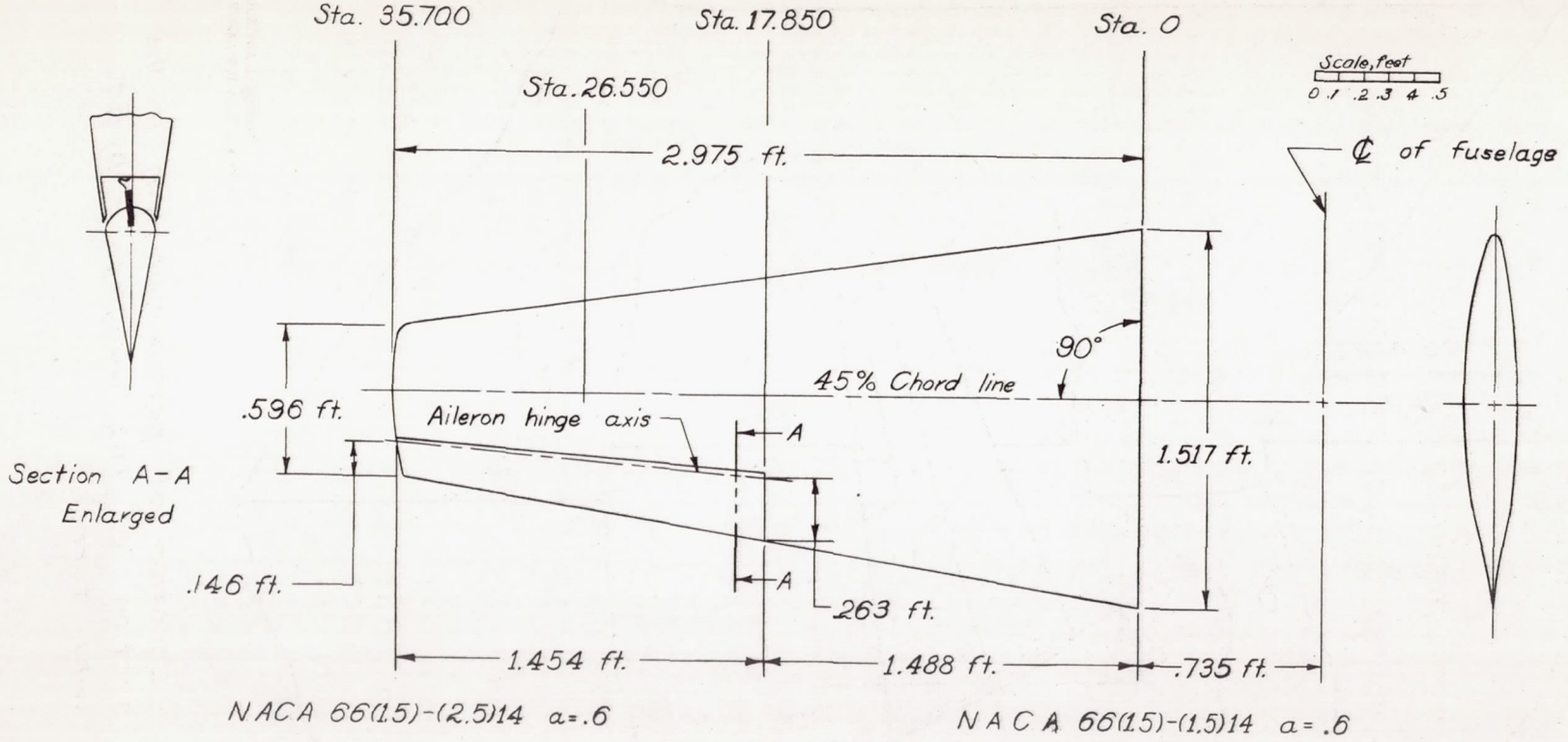

Figure 1.- Details and dimensions of 0.14-scale model of the XP-83 airplane left wing panel as tested in the Langley 4-by 6-foot wind tunnel.

NATIONAL ADVISORY COMMITTEE FOR AERONAUTICS

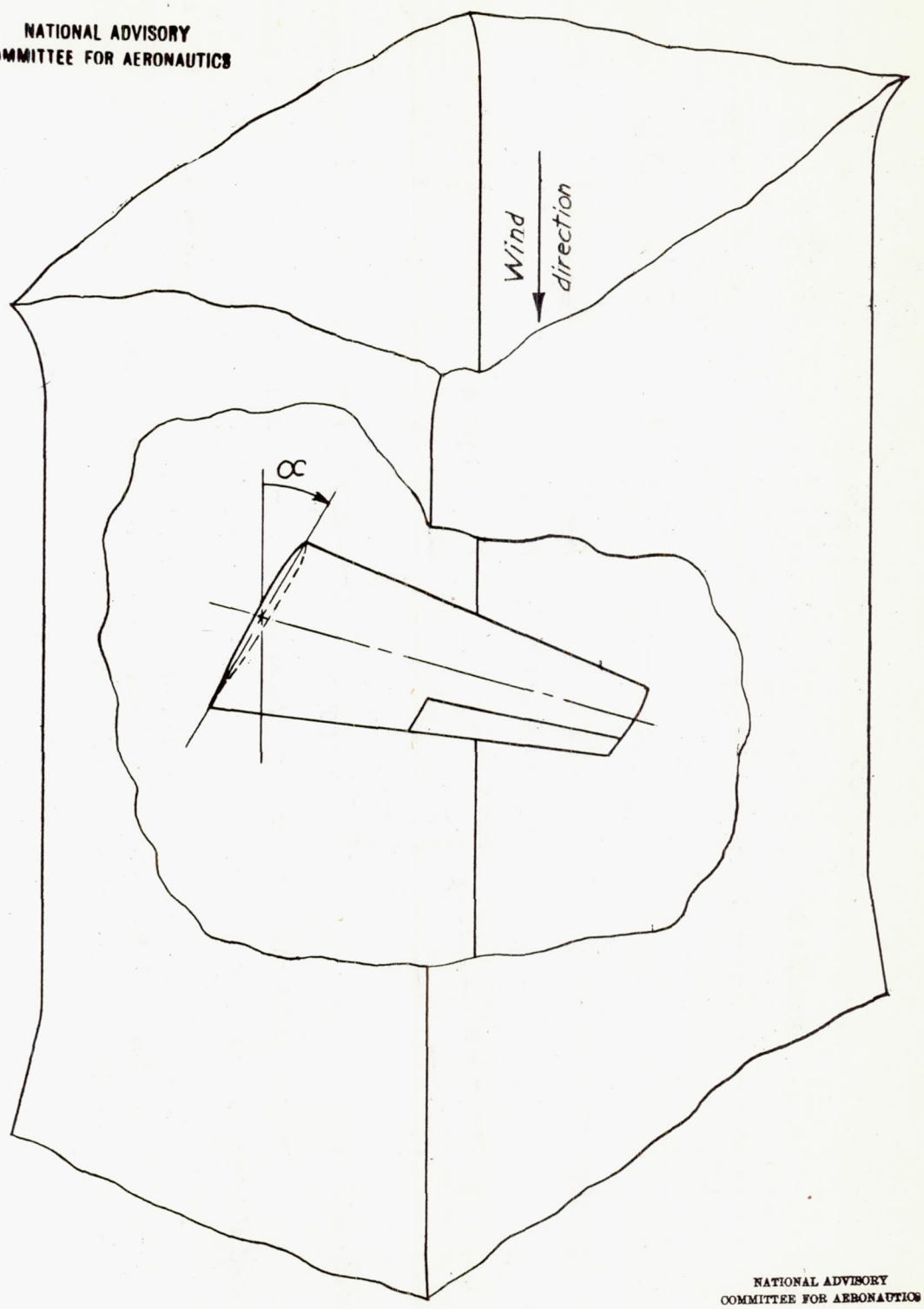

Figure 2.— Location of partial-span wing in the test section of the Langley 4- by 6-foot wind tunnel.

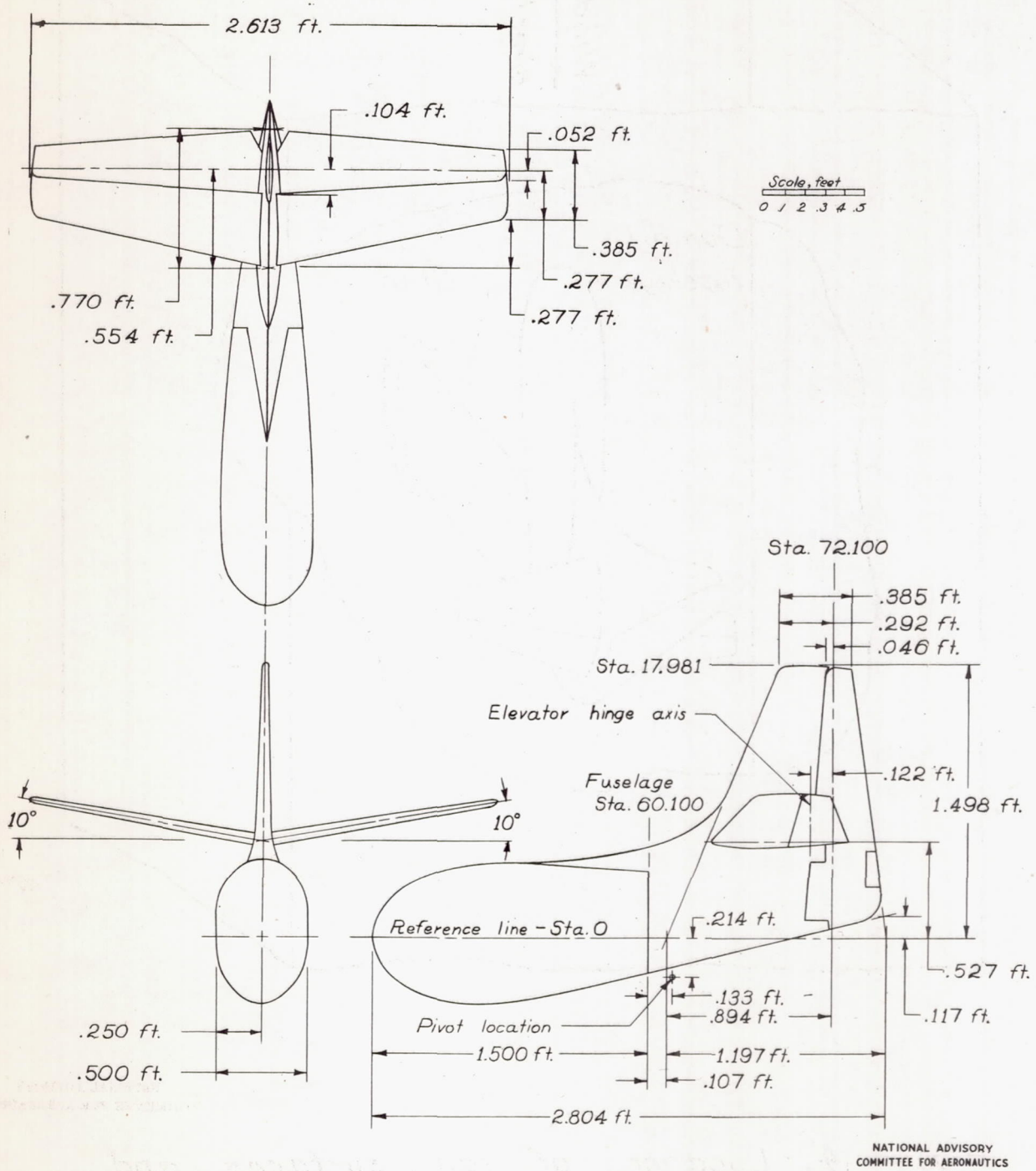

Figure 3 .- Details and dimensions of 0.14-scale model of the XP-83 airplane tail unit tested in the Langley 4-by 6-foot wind tunnel.

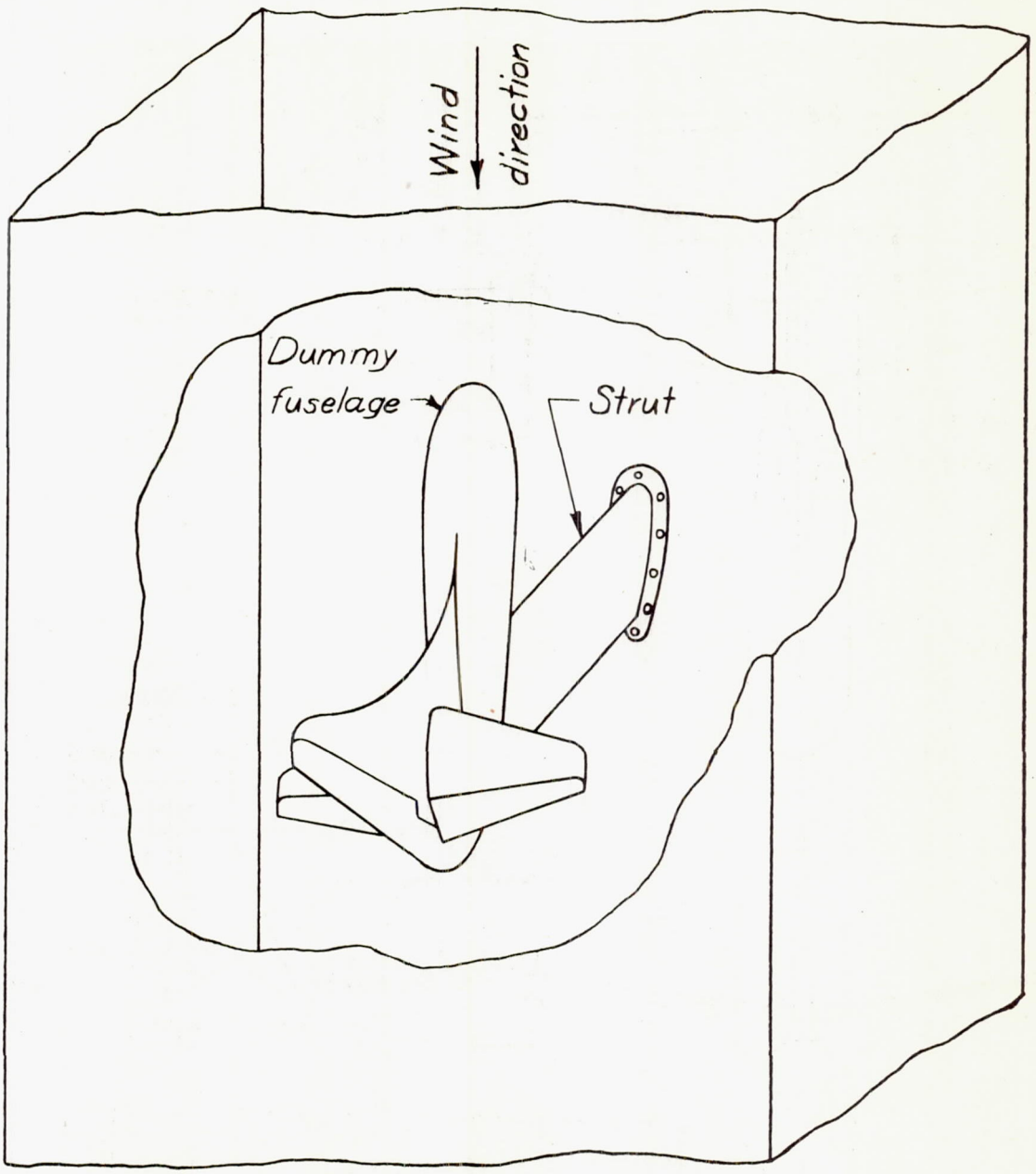

NATIONAL ADVISORY
COMMITTEE FOR AERONAUTICS

Figure 4.- Location of tail surfaces and dummy fuselage in test section of the Langley 4-by 6-foot wind tunnel.

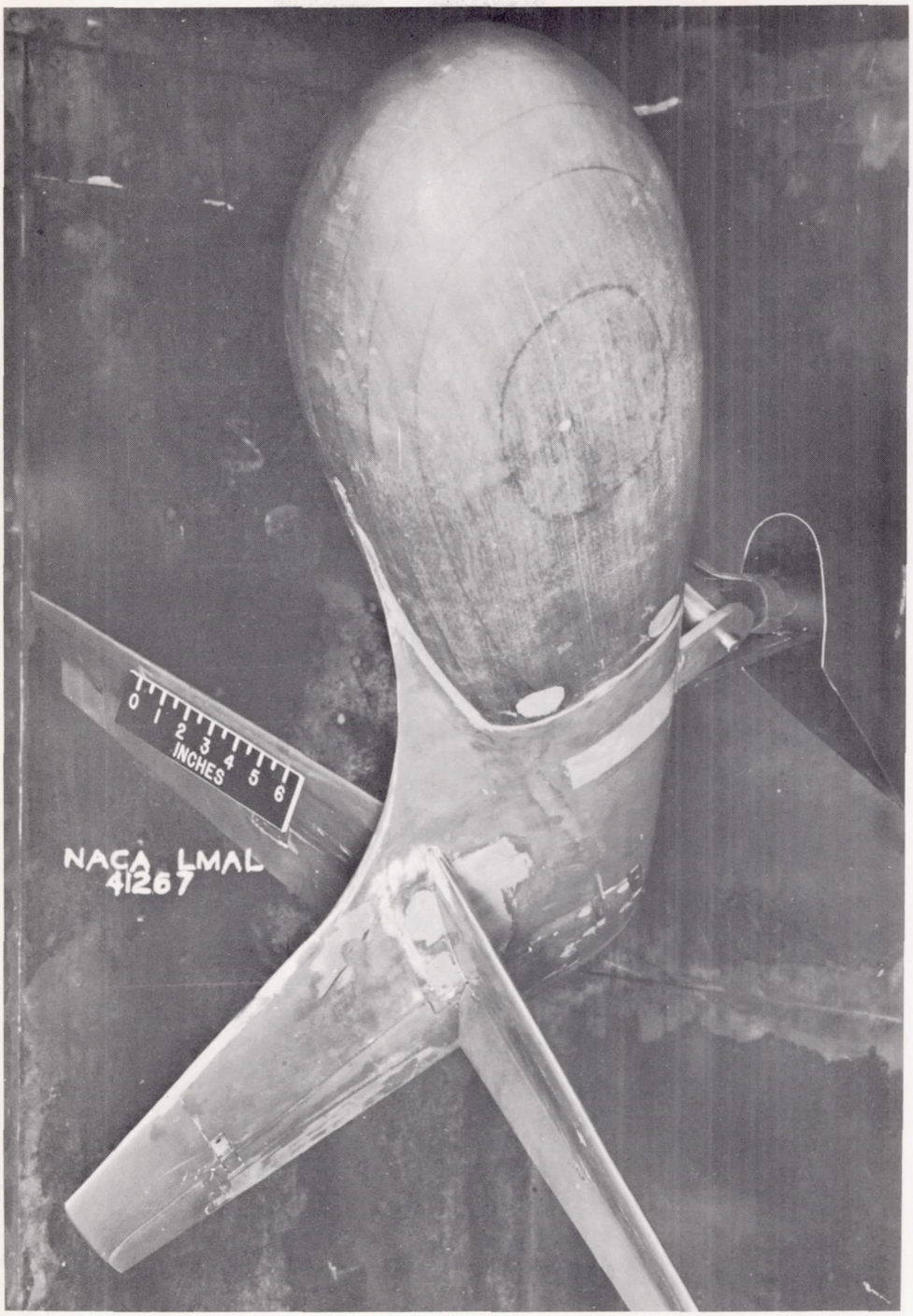

Figure 5.- Three-quarter top view of XP-83 tail surfaces with dummy fuselage as tested in Langley 4- by 6-foot tunnel. Model at positive angle of yaw and at high angle of attack, relative wind vertical in plane of picture.

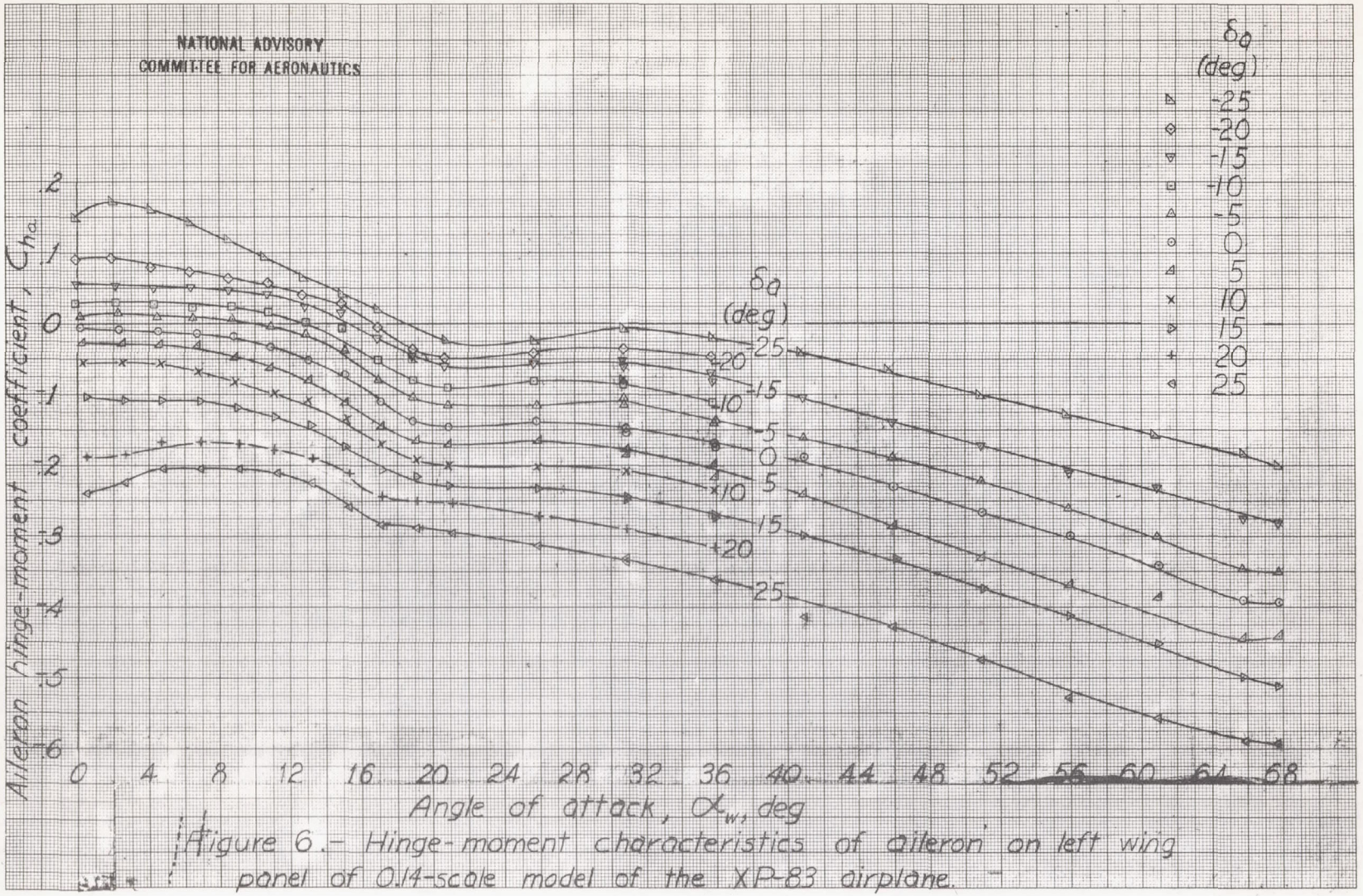

Figure 6.- Hinge-moment characteristics of aileron on left wing panel of 0.14-scale model of the XP-83 airplane.

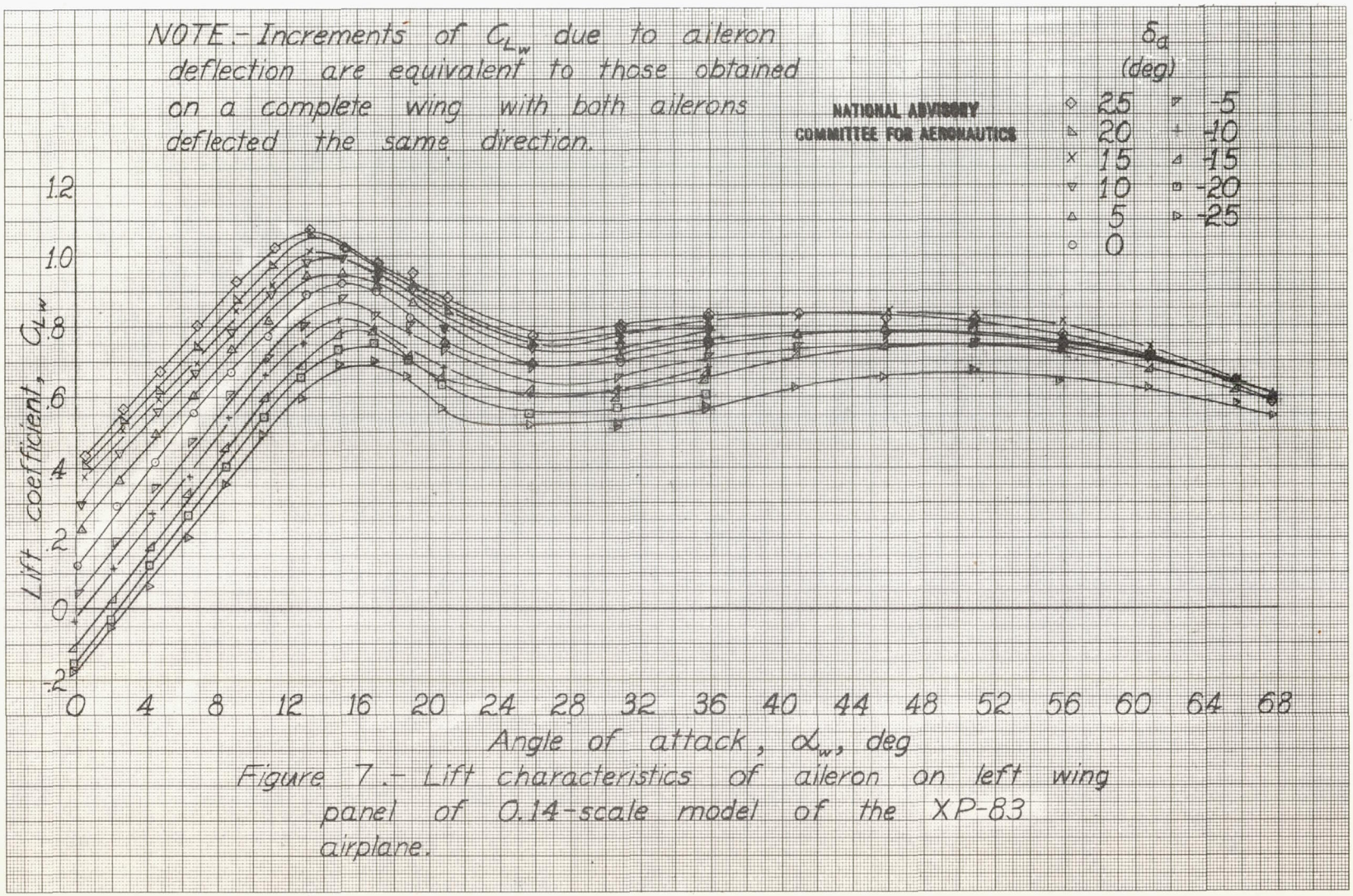

Figure 7.- Lift characteristics of aileron on left wing panel of 0.14-scale model of the XP-83 airplane.

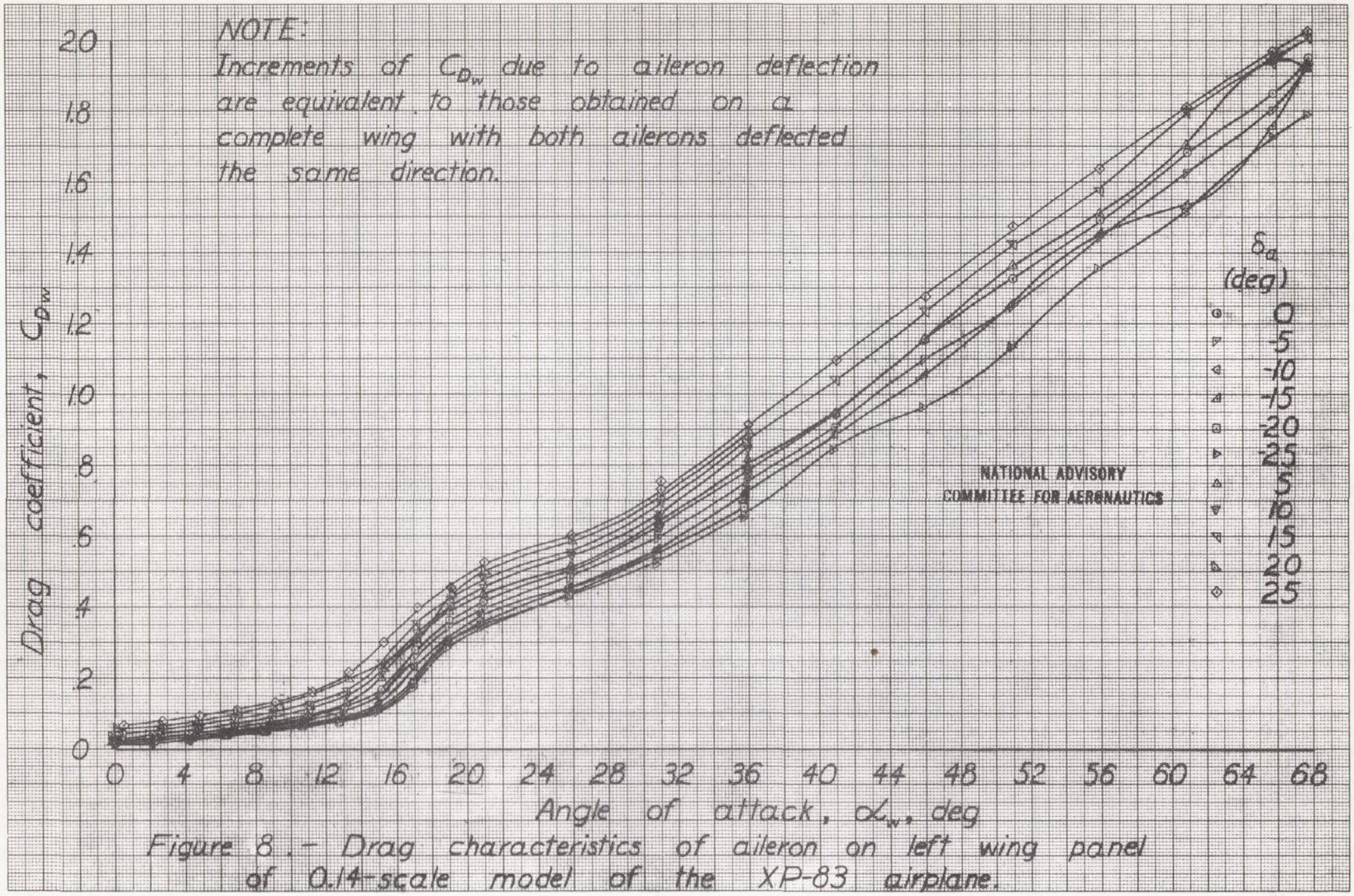

Figure 8.- Drag characteristics of aileron on left wing panel of 0.14-scale model of the XP-83 airplane.

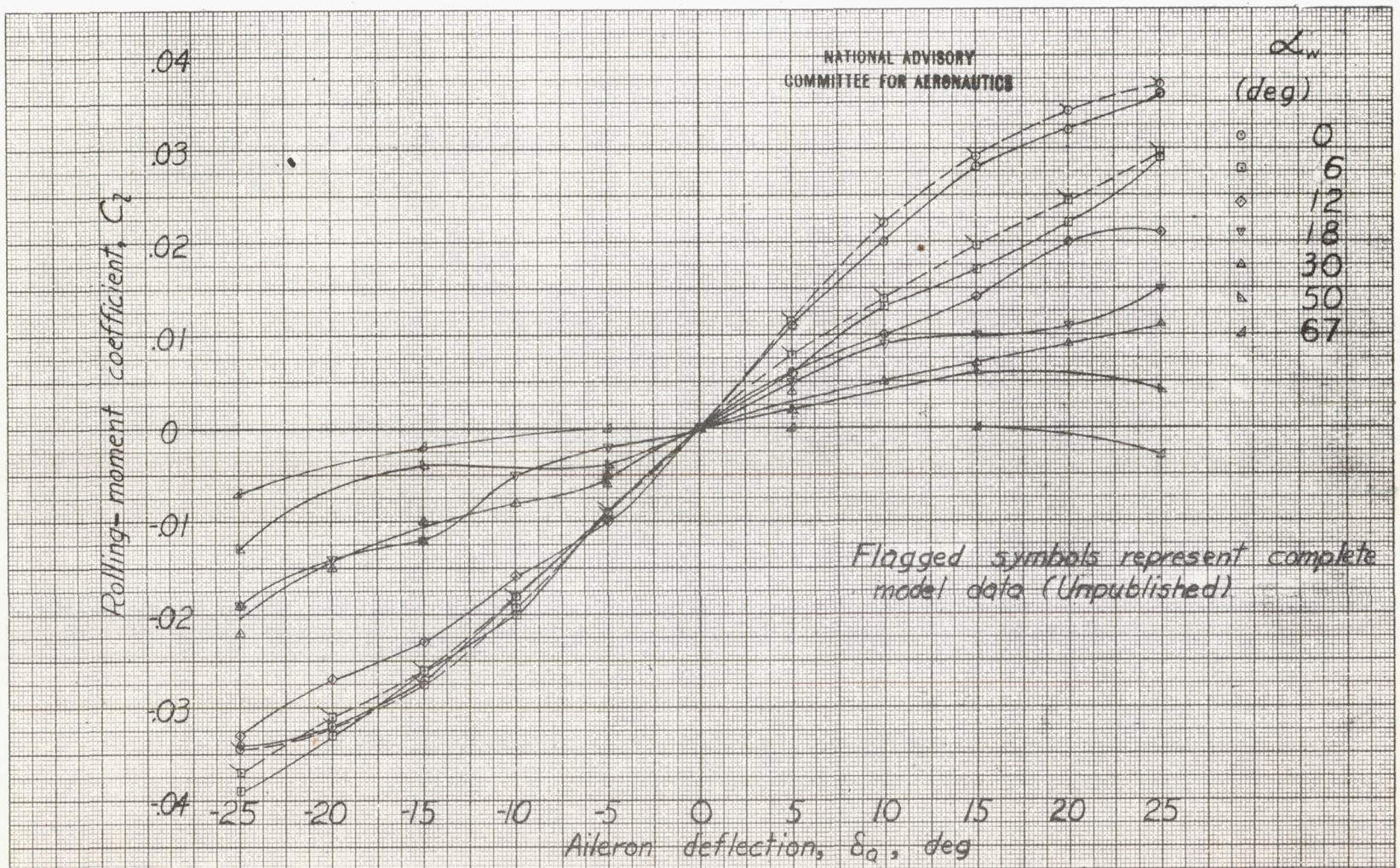

Figure 9.- Rolling-moment characteristics of complete wing of XP-83 airplane with only left aileron deflected, as estimated from left-wing-panel test data.

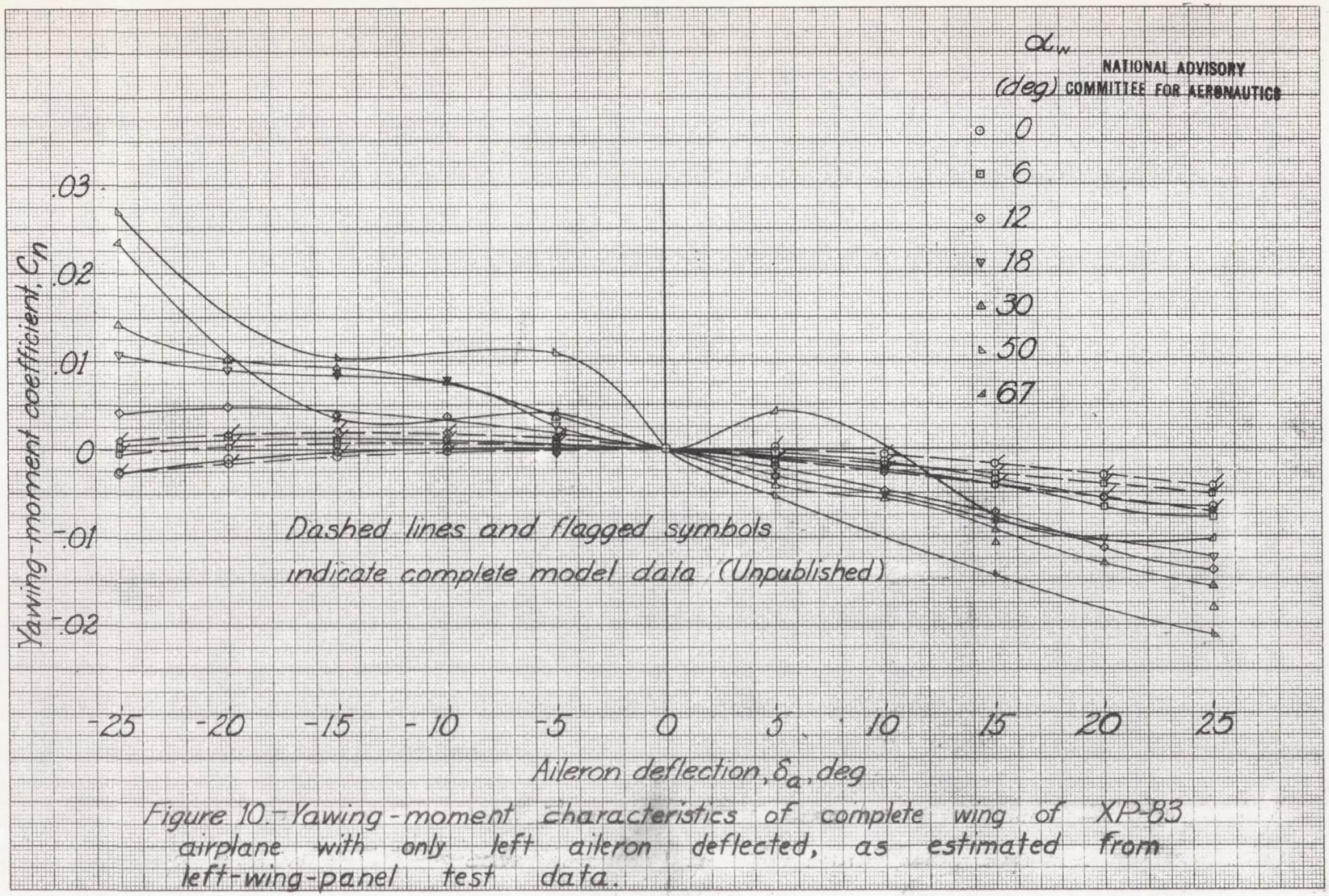

Figure 10.- Yawing-moment characteristics of complete wing of XP-83 airplane with only left aileron deflected, as estimated from left-wing-panel test data.

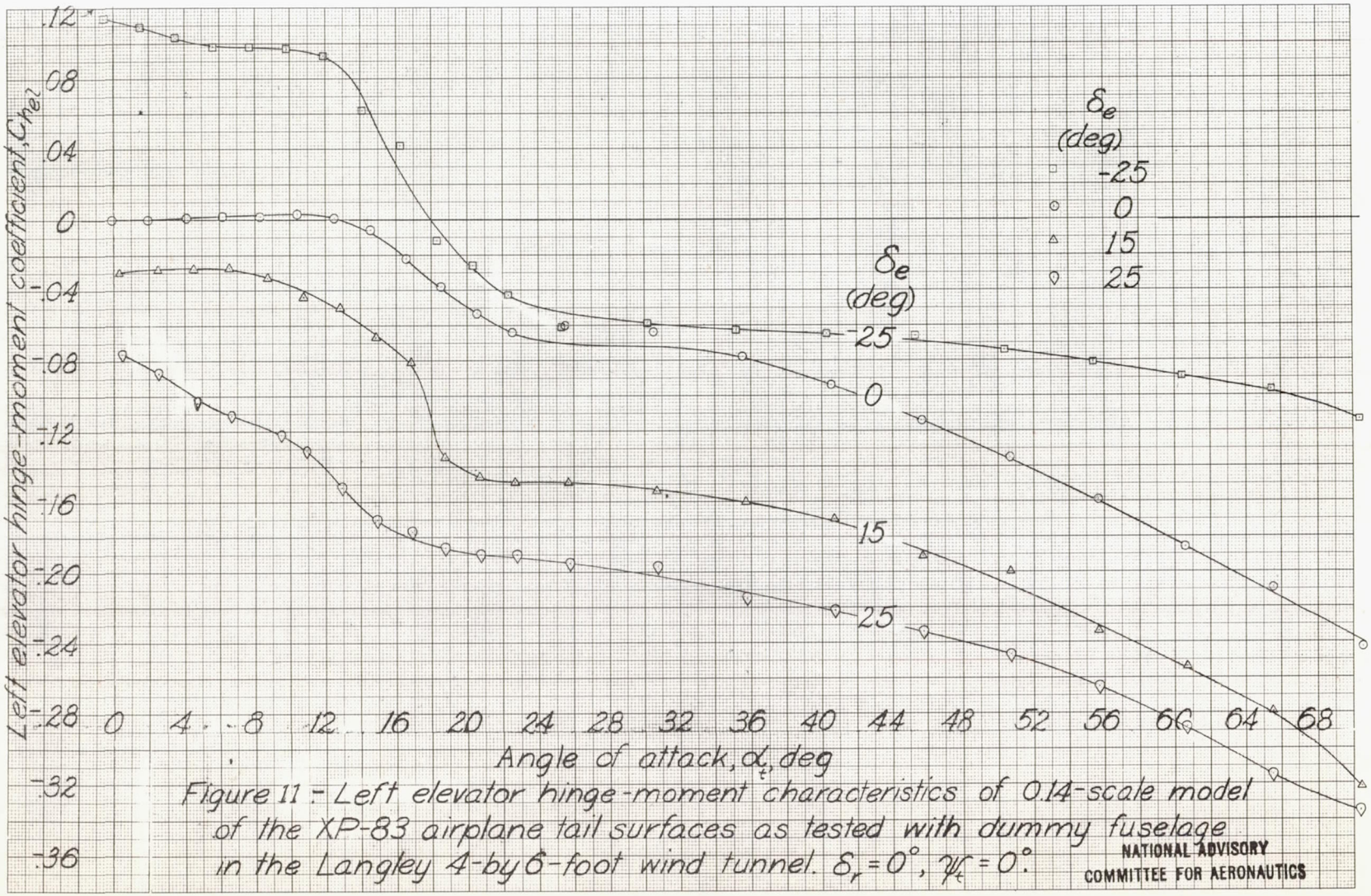

Figure 11 - Left elevator hinge-moment characteristics of 0.14-scale model of the XP-83 airplane tail surfaces as tested with dummy fuselage in the Langley 4-by 6-foot wind tunnel. $\delta_r = 0°$, $\psi_t = 0°$.

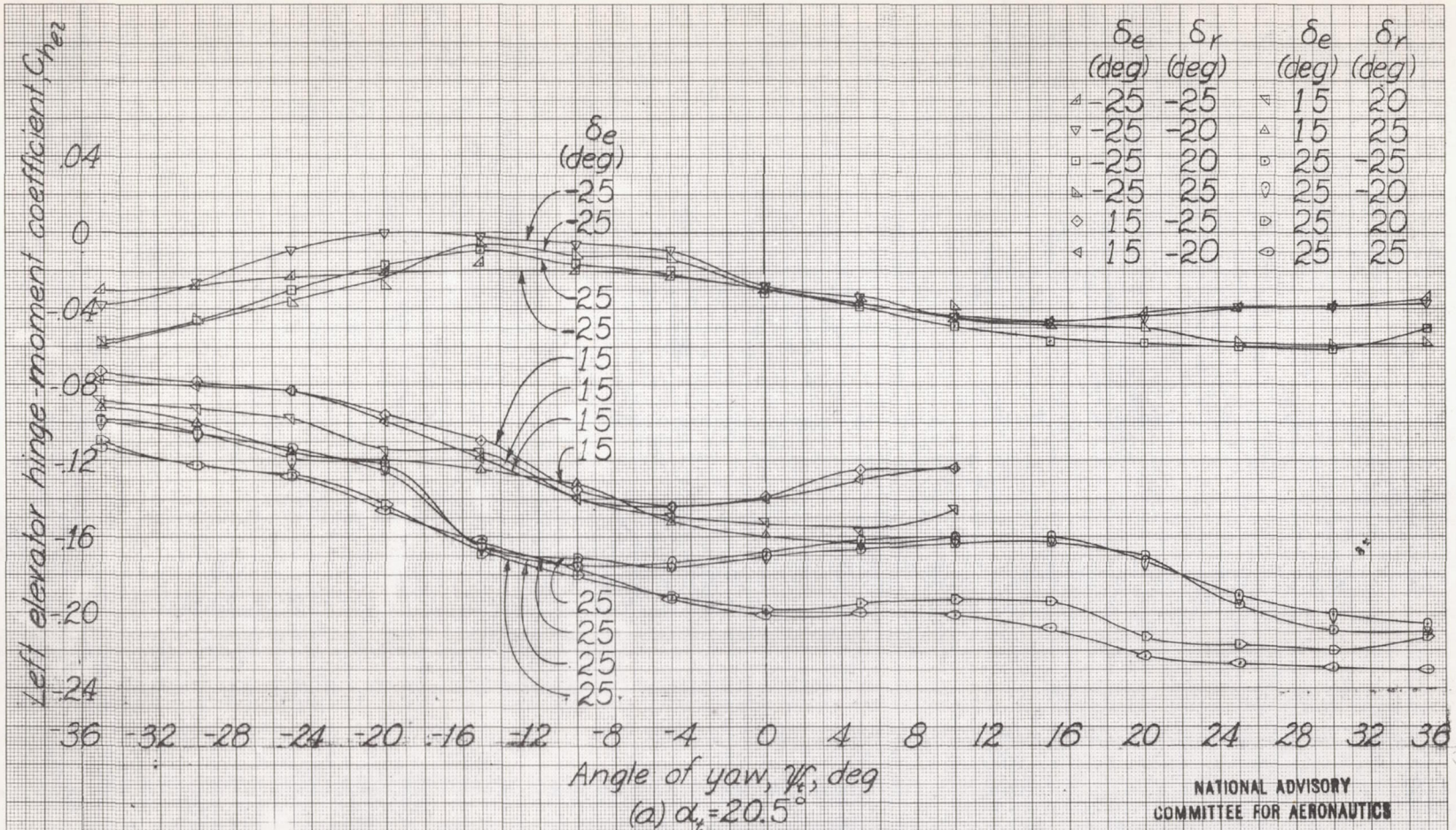

Figure 12.- Left elevator and rudder hinge-moment characteristics of 0.14-scale model of the XP-83 airplane tail surfaces as tested in the Langley 4- by 6-foot wind tunnel.

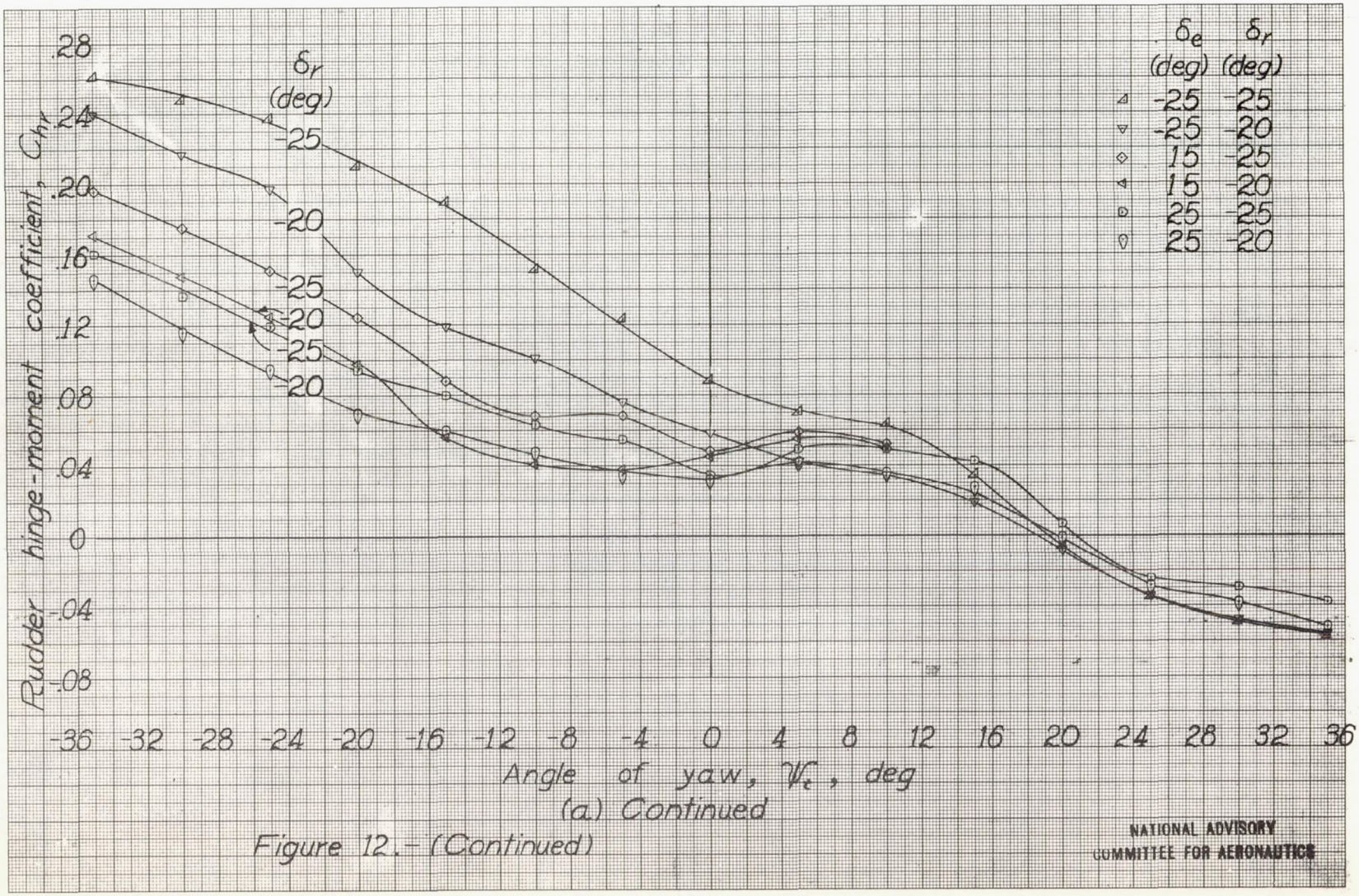

Figure 12.- (Continued)

NATIONAL ADVISORY COMMITTEE FOR AERONAUTICS

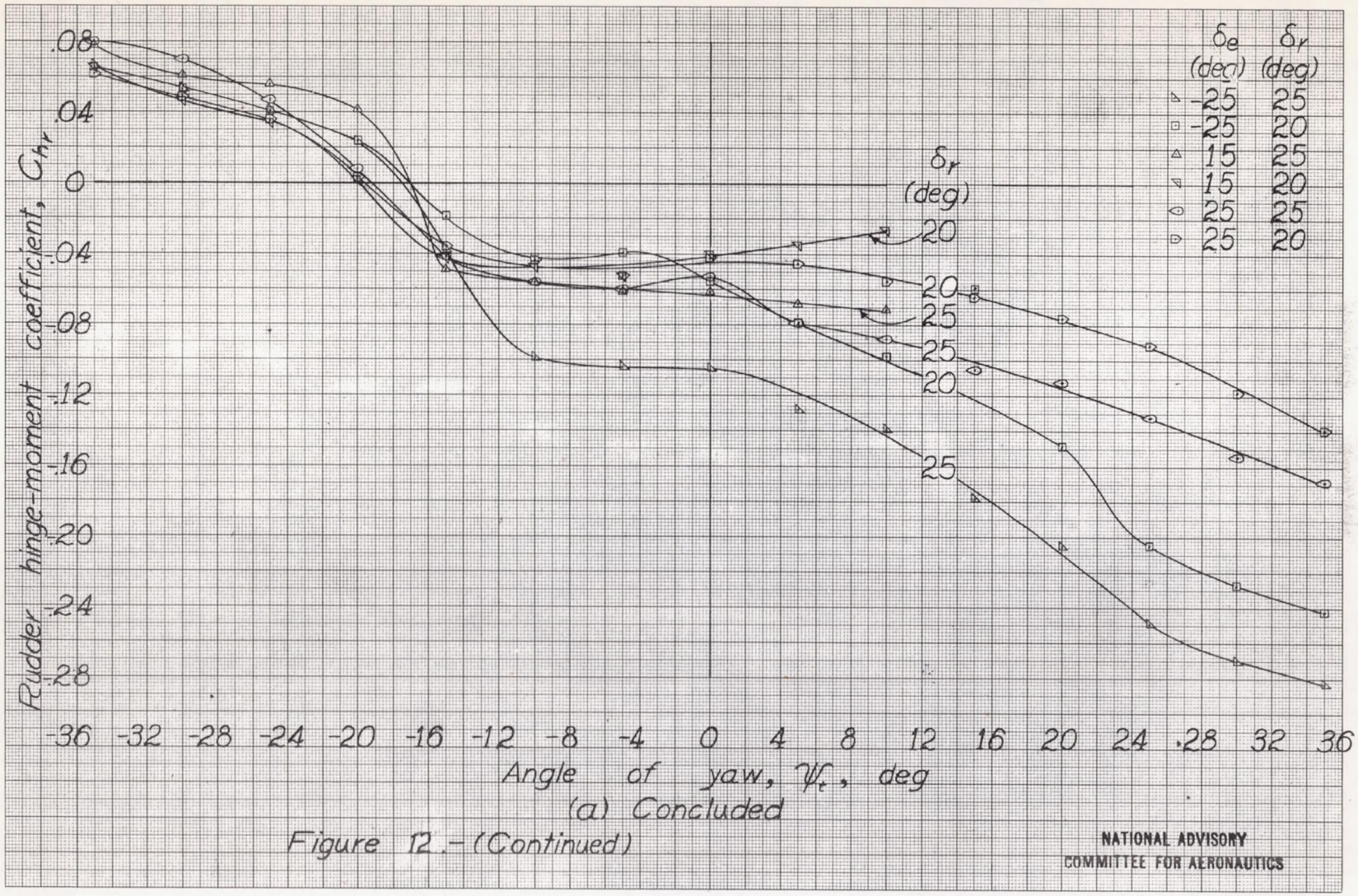

(a) Concluded

Figure 12.- (Continued)

NATIONAL ADVISORY
COMMITTEE FOR AERONAUTICS

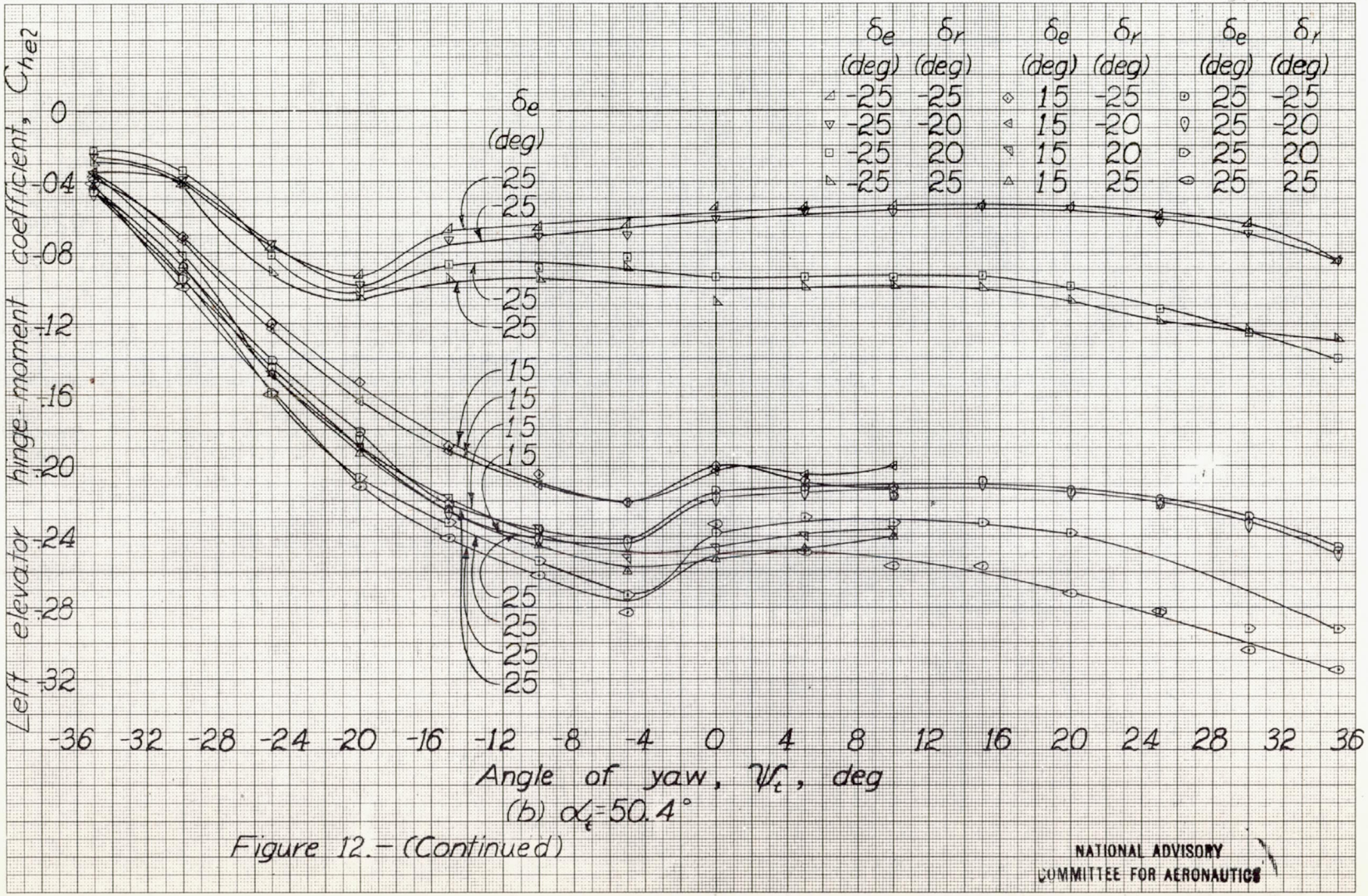

(b) $\alpha_t = 50.4°$

Figure 12.– (Continued)

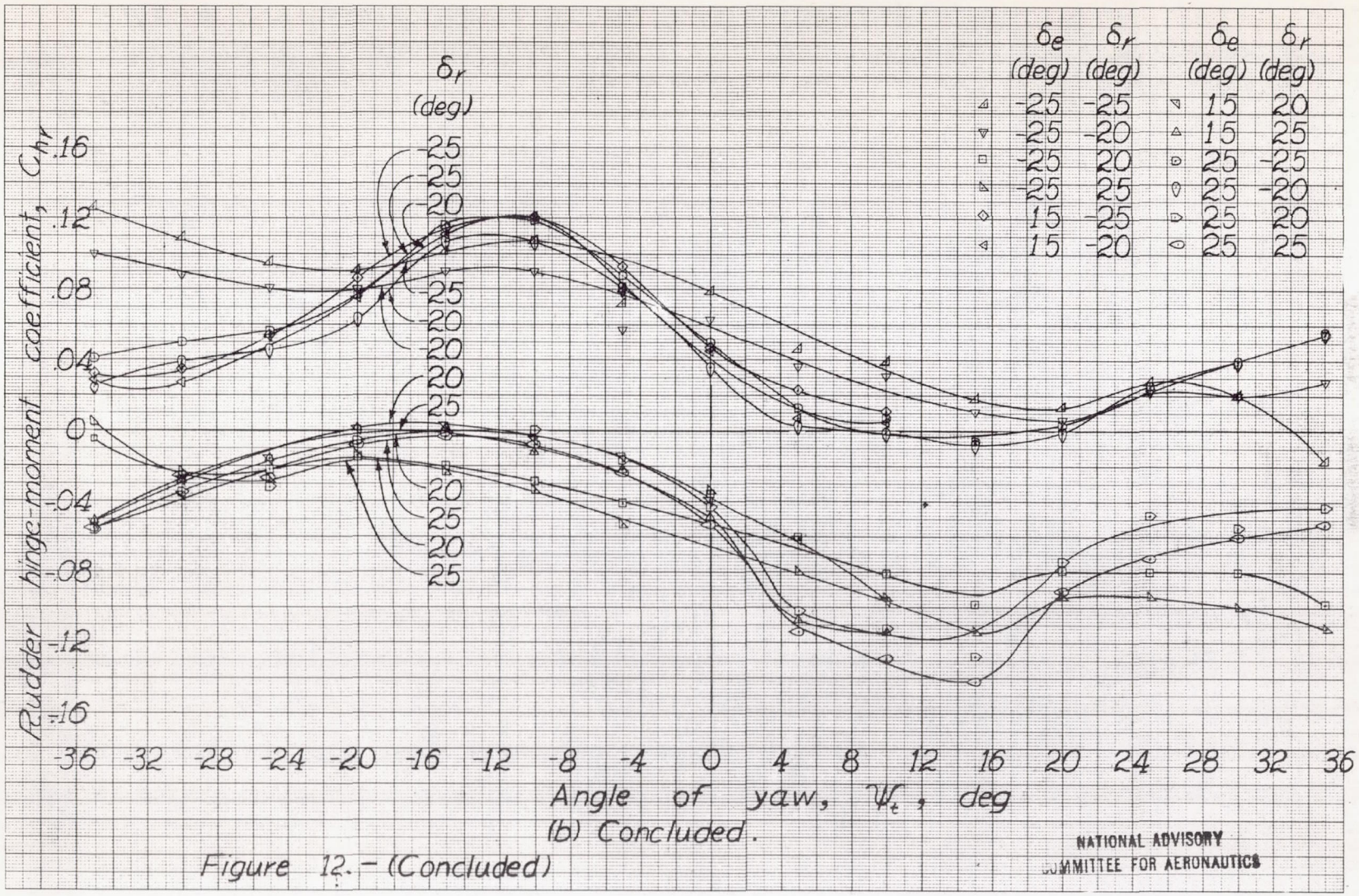

(b) Concluded.

Figure 12.- (Concluded)

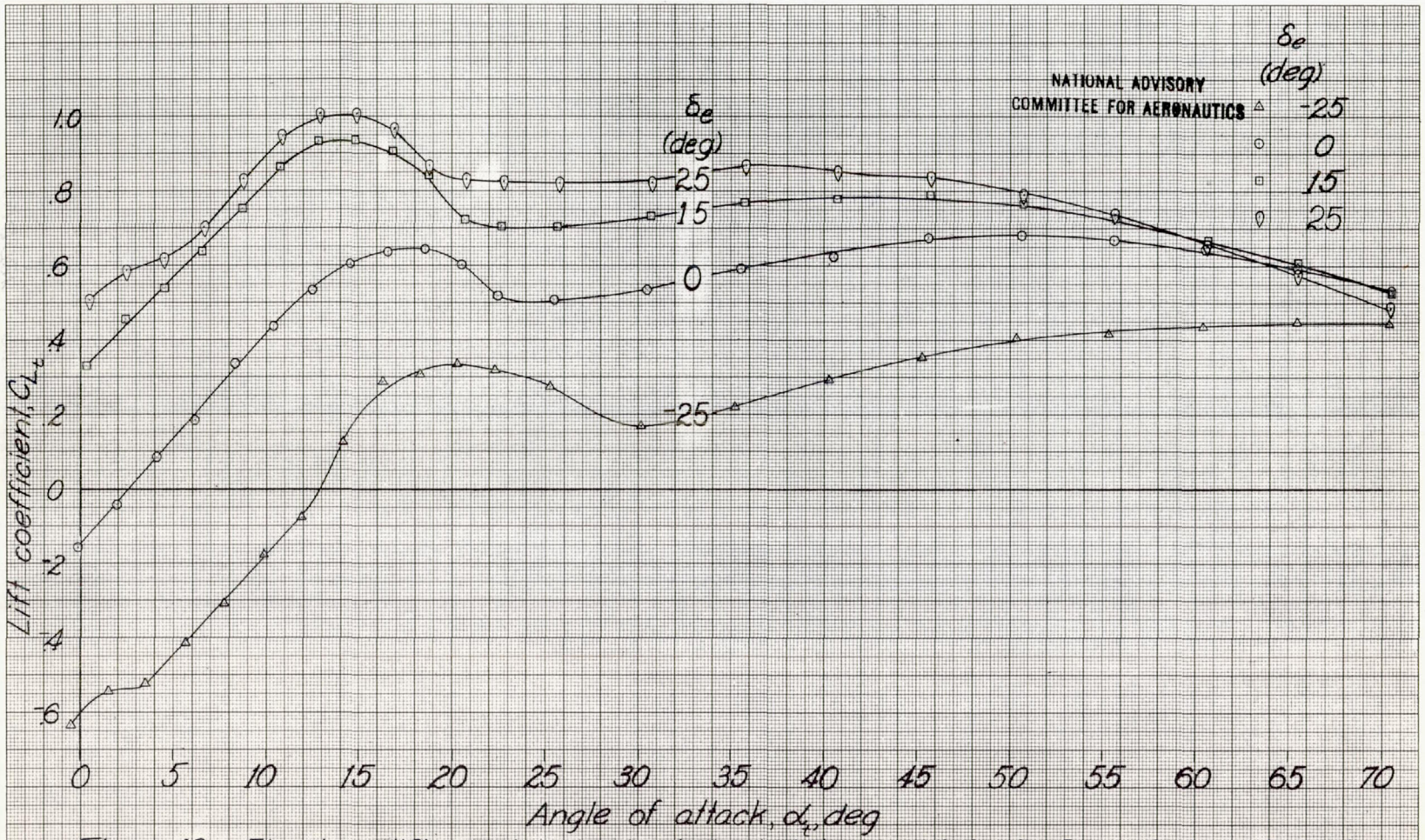

Figure 13.- Elevator lift and drag characteristics obtained from tests of 0.14-scale model of the XP-83 airplane tail surfaces (with fuselage interference) in the Langley 4-by 6-foot wind tunnel. $\delta_r = 0°$, $\psi_t = 0°$.

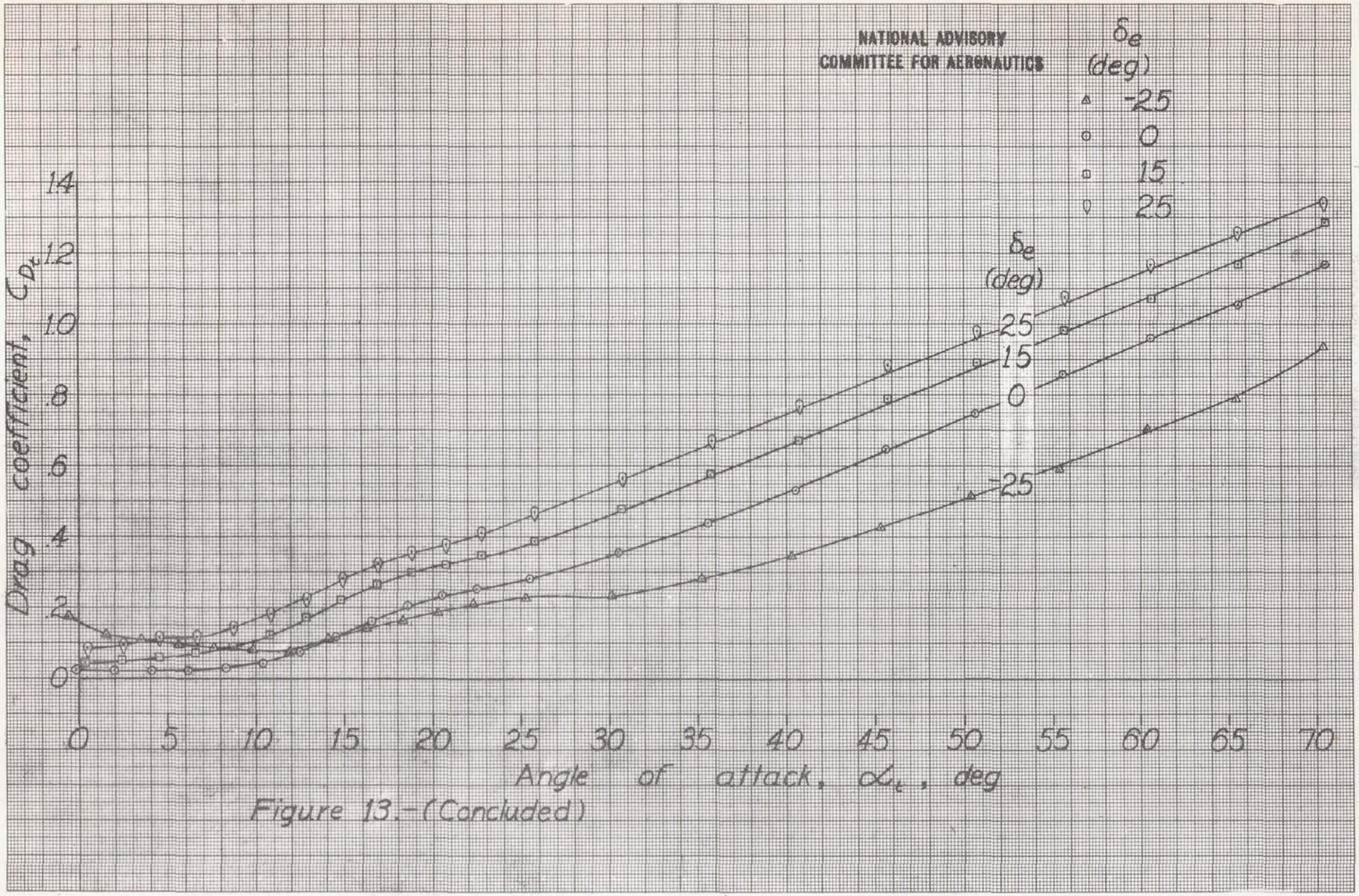

Figure 13.- (Concluded)

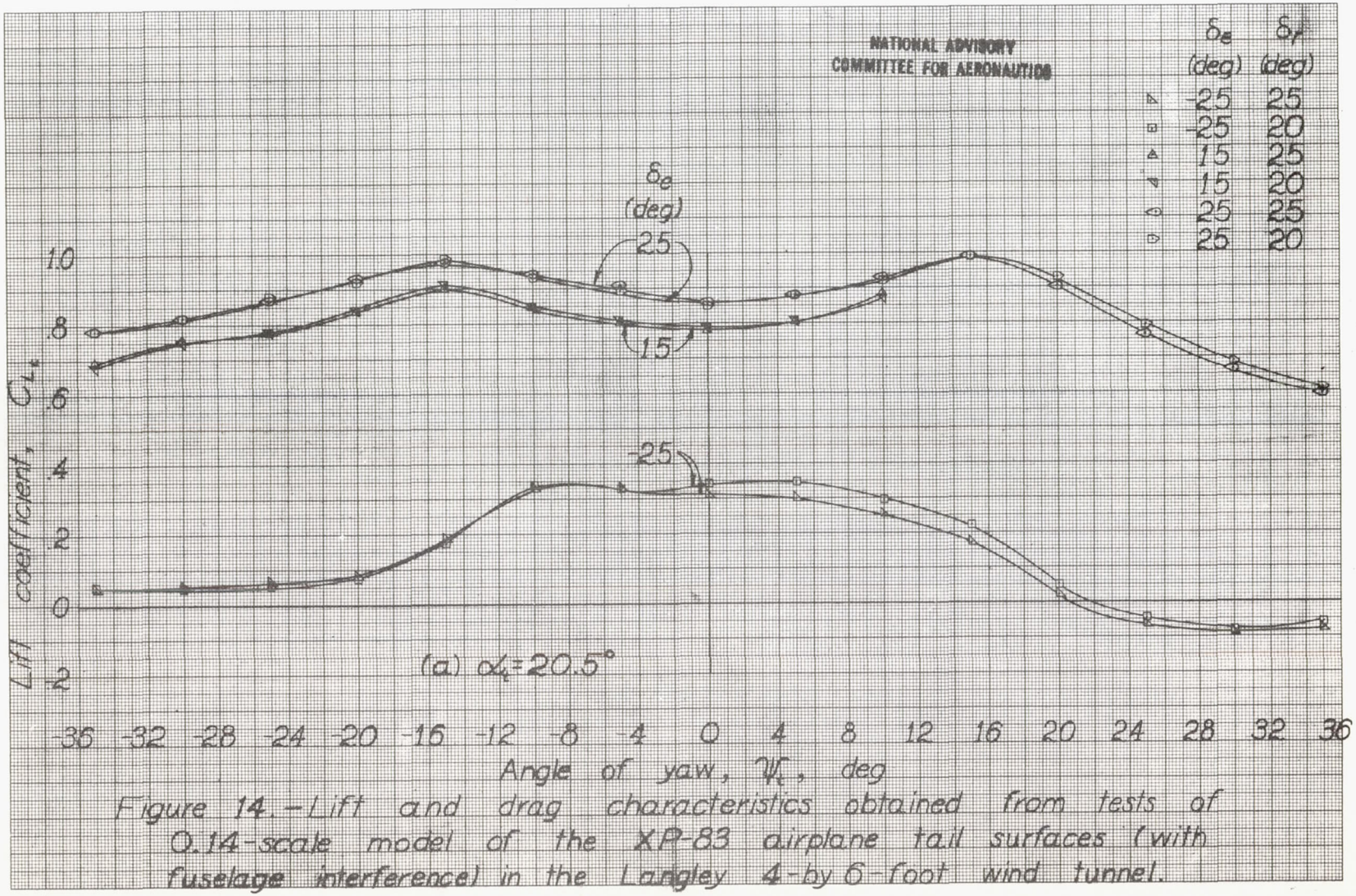

Figure 14.–Lift and drag characteristics obtained from tests of 0.14-scale model of the XP-83 airplane tail surfaces (with fuselage interference) in the Langley 4-by 6-foot wind tunnel.

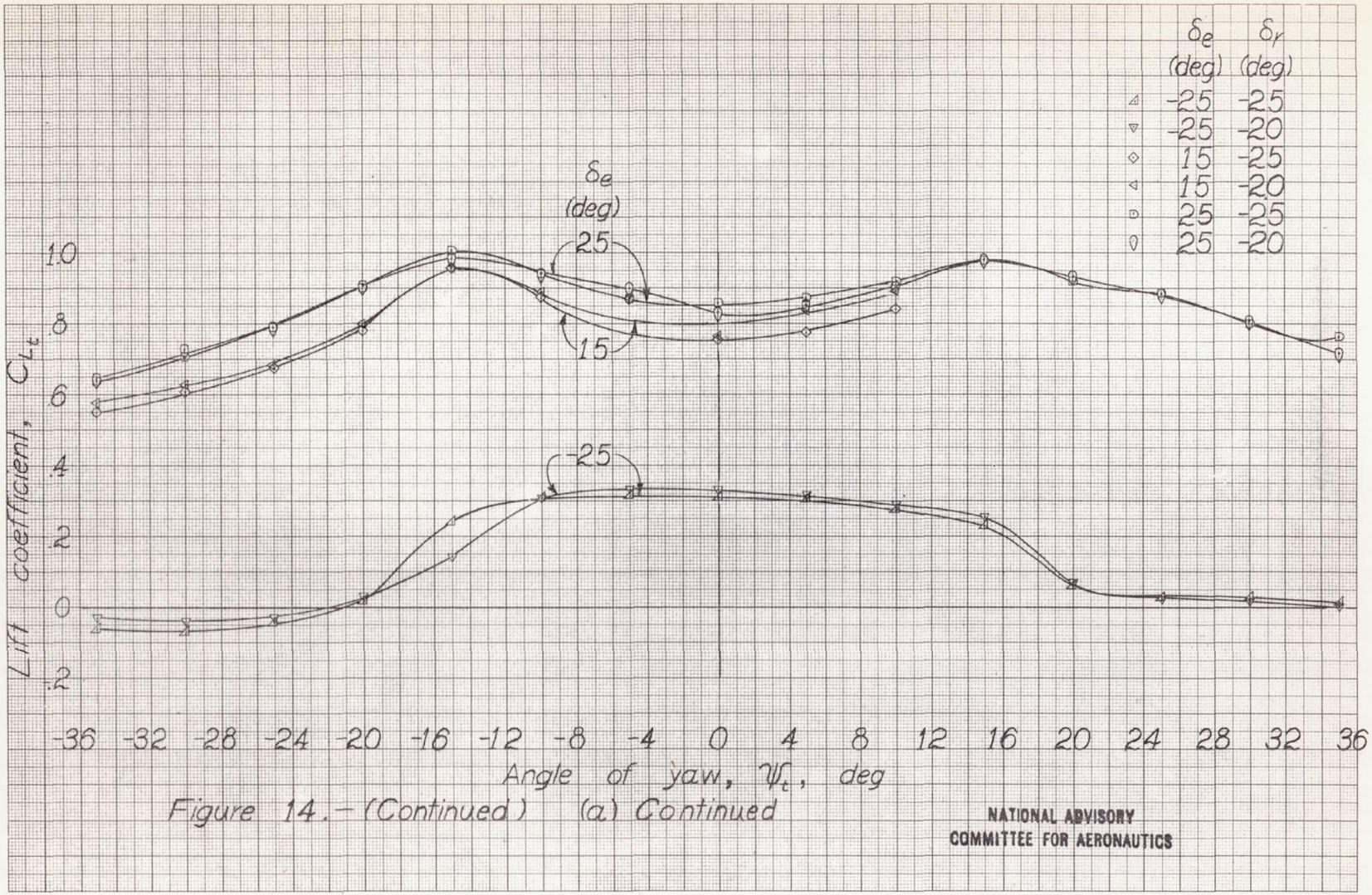

Figure 14.- (Continued) (a) Continued

NATIONAL ADVISORY
COMMITTEE FOR AERONAUTICS

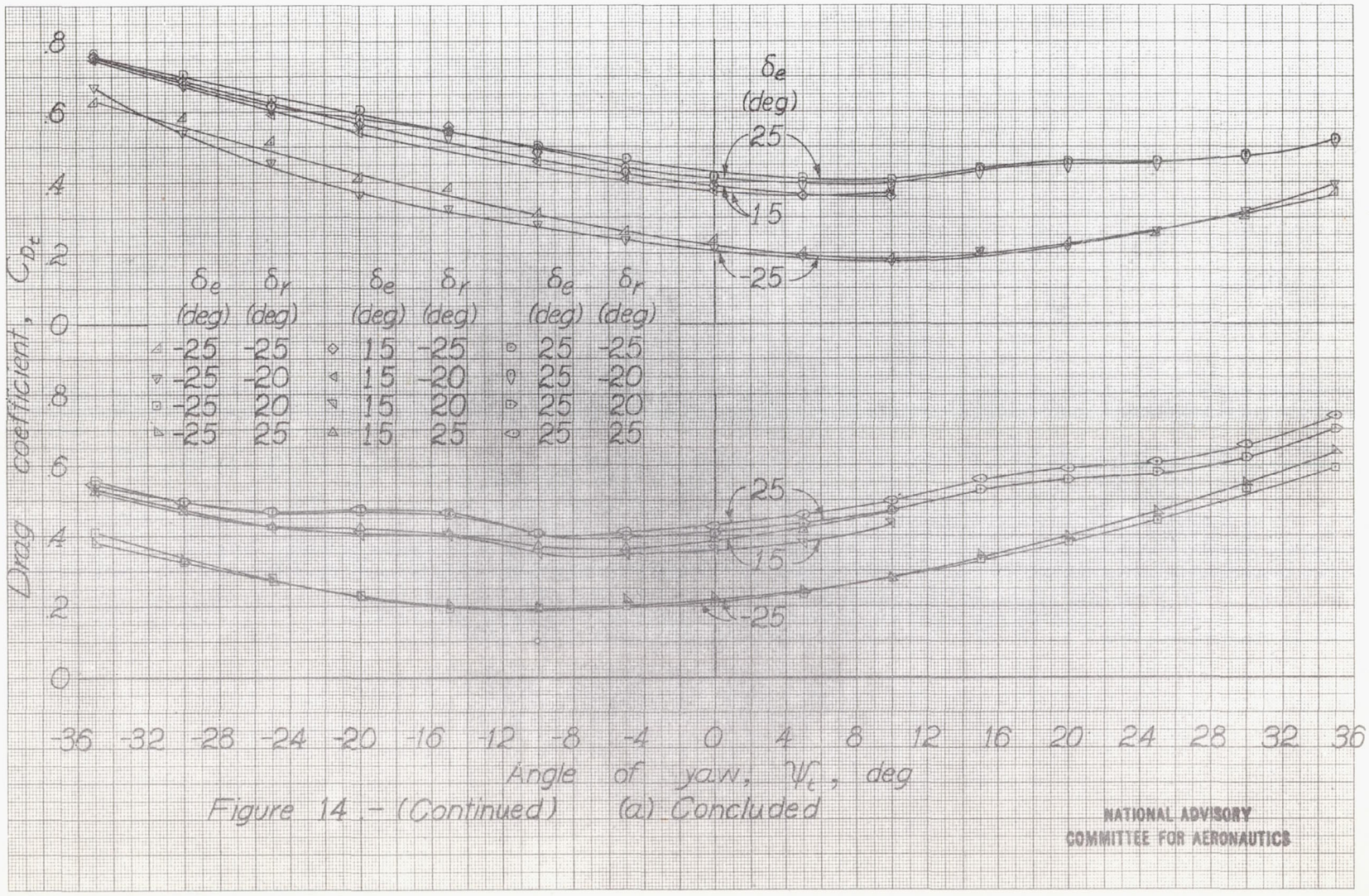

Figure 14.- (Continued) (a) Concluded

NATIONAL ADVISORY
COMMITTEE FOR AERONAUTICS

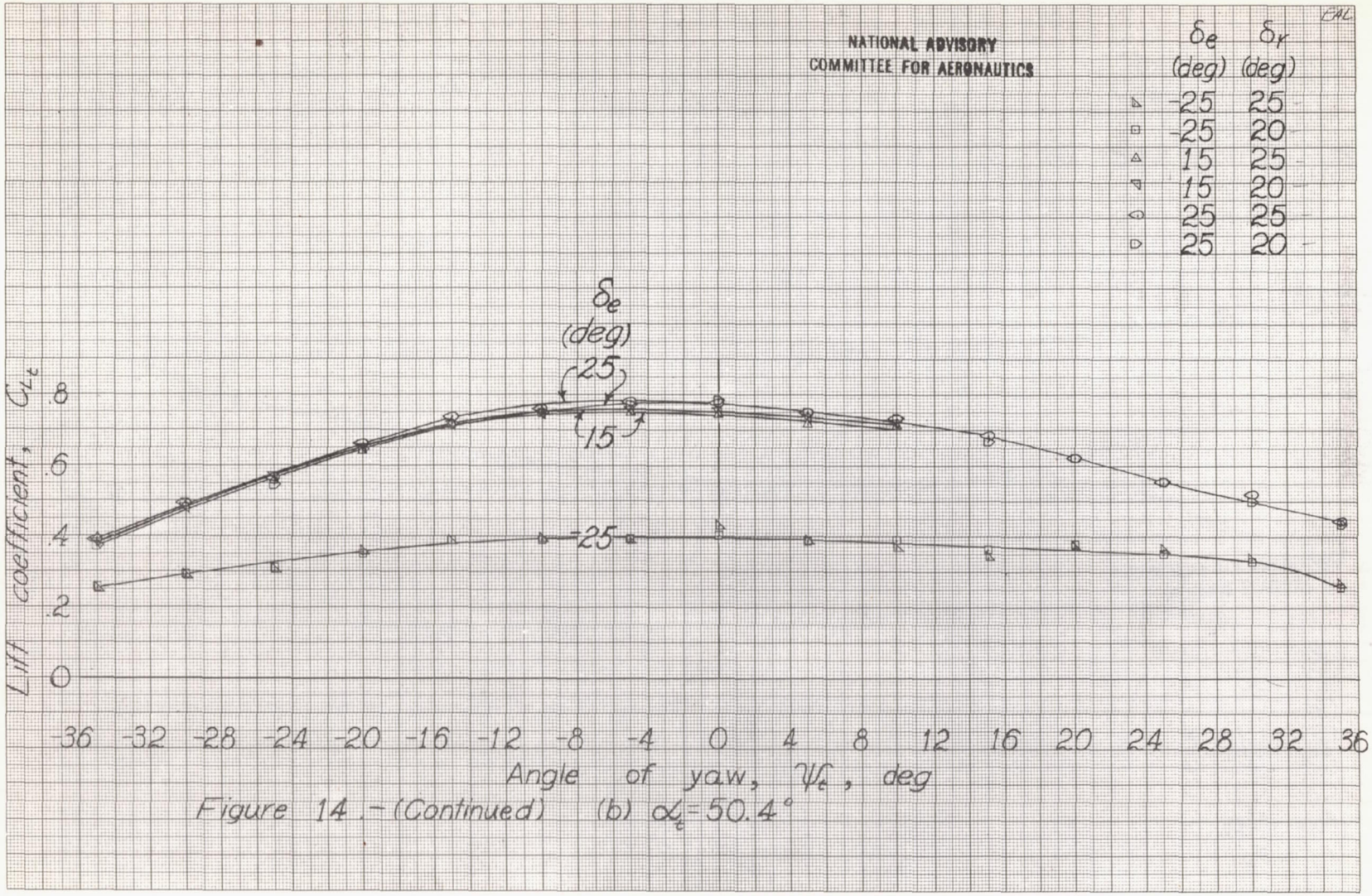

Figure 14.- (Continued) (b) $\alpha_t = 50.4°$